17 Pharmacodynamics

INDRANIL RAO[1,2], VINAY HK[1,2] and SANDHYA MANDLEKAR[1,3]

[1]Biocon Bristol-Myers Squibb R&D Center (BBRC), Bangalore, India
[2]Syngene International Ltd., Bangalore, India
[3]Bristol-Myers Squibb India Pvt. Ltd., Bangalore, India

17.1 SUMMARY

Pharmacodynamics (PD) is the study of physiological effects of drugs on the body and their mechanisms of actions. It provides the basis for rational therapeutic use of drugs and the design of new and superior therapeutic agents [1]. PD comes from the Greek word for "drug," "pharmakon," and dynamics means "variation in intensity." On the other hand, pharmacokinetics (PK) deals with how the body handles the drug after it is absorbed and involves disposition, that is, distribution, metabolism, and excretion processes. For example, an orally administered anticonvulsant drug has to enter the brain after crossing intestinal, hepatic, and blood–brain barriers. The drug has to reach its site of action (brain) in sufficient concentrations and duration to interact with a specific target (i.e., receptor) to produce the desired effect. The drug concentration measured in plasma is more reflective of drug concentration at the site of action than dose, because the dose–response relationship is confounded by PK variables, including

Encyclopedia of Drug Metabolism and Interactions, 6-Volume Set, First Edition.
Edited by Alexander V. Lyubimov.

bioavailability, nature of dose–concentration relationships, and formation of active metabolites.

The effect of the drug can be measured as a clinical end point or using a biomarker. The effect of the drug on clinical end point may require studies of extended duration to manifest, for example, increase in survival time, prevention of stroke, and prevention of bone fracture. In these situations, biomarkers may help track the progress of therapy. For example, in the case of an antihypertensive drug trial, blindness, renal failure, and premature mortality can serve as clinical end points and can be measured after prolonged treatment. A simpler biomarker would be blood pressure changes, which are reduced by treatment with an antihypertensive drug. Adiponectin, blood glucose, or binding of a positron emission tomography (PET) ligand to a specific receptor could also serve as biomarkers to evaluate target modulation by a drug candidate. Other PD measures such as QT interval, liver function tests, and white blood cell count can serve as safety biomarkers.

Quantitation of dose–effect relationship was started in 1910 by Hill [2] when he described the association of hemoglobin and oxygen using a relationship that is more widely known as the *Hill equation*. The $E_{\max}$ model used commonly in all PD models was derived from the Hill equation [3]. This concept was first applied by Clark [4] to evaluate the dose–effect relationship of drugs. The hyperbolic nature of the function describes lack of a dose proportional effect after a given dose. Quantitative analysis of the dose–effect relationship has evolved over the years. A significant advancement in PD modeling was to link the PK and PD models to have a better understanding of the time course of PD effect [5]. Another advancement in PD modeling was a method to account for temporal delay observed in pharmacological response when compared to plasma concentrations [6]. Over the years, many types of mechanistic PD models have led to better understanding of different biomarkers and the importance of measuring the right biomarker to predict the clinical response and aid in the design of better clinical trials.

In this chapter, we describe the basic tenets of pharmacodynamics (drug–receptor interactions and agonists vs antagonists), the relative importance of biomarkers, and provide a summary of basic PD models reported in the literature.

17.2 MECHANISMS OF DRUG ACTION

Pharmacological response is initiated by the interaction between a drug and a binding site on a macromolecule in a tissue. This macromolecule is known as the *drug receptor*. The drug–receptor interaction results in a cascade of different steps within the cell, which ultimately leads to a physiological response:

$$\text{Drug} + \text{receptor} \underset{k_{-1}}{\overset{k_1}{\rightleftharpoons}} \text{drug} - \text{receptor complex} \rightarrow \text{transduction pathway} \rightarrow \text{response}$$

Receptor is a cellular macromolecule or an assembly of macromolecules, which is concerned directly and specifically with chemical signaling between and within cells [7]. Most receptors are proteins (>90%), except some targets such as DNA. These receptors act as a recognition site and messenger to transfer information from the

outside of the cell to the cytosol. The regulatory effects of a receptor may be exerted directly on its cellular targets, effector proteins, or may be conveyed by intermediary cellular signaling molecules called *transducers*. The receptor, its cellular target, and any intermediary molecules are referred to as *mediators* of the signal-transduction pathway. Frequently, the proximal effector protein is not the ultimate target but rather is an enzyme or transport protein that creates, moves, or degrades a small metabolite (e.g., a cyclic nucleotide) or ion (e.g., Ca^{2+}) known as *second messenger*, which will convey information to a variety of targets. The detailed understanding of the signal-transduction pathways helps us design better molecules that interact with different cellular targets to modify physiological and/or pathological processes. It is very challenging to establish that a certain molecular interaction is indeed the one triggering the particular effect. In this respect, genetically modified models such as receptor knock-out animals are proving increasingly useful. For example, a lack of effect of a drug in mice lacking a particular target can provide strong support that the effects of the drug are mediated by that particular target [8].

The cellular proteins are either human genome-derived proteins or belong to pathogenic organisms. In 2002, after sequencing of the human genome, approximately 8000 targets of pharmaceutical interest were estimated. Only a small fraction of those targets is modulated by approved drugs. In 2006, Imming *et al*. catalogued 218 molecular targets for approved drug substances under different target families: enzymes, G-protein-coupled receptors (GPCRs), nuclear hormone receptors, cytokine receptors, ion channels, transport proteins, and so on. Altogether, it suggests that a very large number of putative drug targets remain to be explored [9,10].

During the process of drug discovery, the discovery teams design potential drug candidates that will have a desired pharmacological effect on the human body. If we look at processes at the molecular level in the human body, we would see multiple simultaneous chemical reactions taking place, keeping the systems healthy and functional. The administered agent on reaching its target site will interfere with these chemical reactions to produce a specific effect. The interaction of a drug with a macromolecular target involves a process known as *binding*. There are usually specific areas in the macromolecule where interactions take place, and they are known as the *binding sites*. The interaction of the drug with its target is mediated through electrostatic or ionic bonds, hydrogen bonds, van der Waals interaction, dipole–dipole interactions, and hydrophobic interactions. None of these bonds is as strong as the covalent bond that makes the structure of the molecule, and so they can form and get dissociated. This means that equilibrium is reached between the bound and unbound drugs and its target. Drugs having a large number of interactions are likely to remain bound longer than those that have only a few. Few drugs form irreversible covalent bonds with their receptor. For example, aspirin binds covalently to cyclooxygenase enzyme and prevents formation of thromboxane. The effect will continue until new cyclooxygenase enzyme is synthesized. Other examples include proton pump inhibitors (e.g., omeprazole) that bind irreversibly to H^+ K^+-ATPase pumps and block gastric acid secretion.

When the drug molecule combines with the receptor, there might be a delay in the response depending on the nature of the signal-transduction pathway. Thus, for ion channel opening, the delay is only milliseconds, while for DNA transcription, the delay may be in hours to days. This information is very useful while building the relationship between the concentration and effect for a drug. Cells in different tissues may have multiple receptors, each of which is specific for a particular ligand. For example, on the

myocardial cell, there are β-receptors, muscarinic receptors, and multiple ion channels. Functional groups present in the drug are important in forming intermolecular bonds with the target. However, the carbon skeleton of the drug also plays an important role in binding the drug to its target. Small changes in chemical structure can produce profound changes in potency. For example, codeine, which differs in structure from morphine only by methoxy group instead of a hydroxyl group, is ~1000 times less potent than morphine in its action on opioid pathway (Fig. 17.1).

Each drug may interact with multiple receptor subtypes to different extent. Few drugs may be absolutely specific for one receptor or subtype, but most drug candidates will have relative selectivity. Selectivity is the degree to which a drug acts on a given site relative to other sites. At higher concentrations, the same drug may interact with other targets (receptor subtypes or different targets) leading to undesirable effects.

Some of the major drug targets and signal-transduction mechanisms are briefly discussed below.

17.2.1 Ion Channels

Ion channels are membrane proteins, found virtually in all cells that are of crucial physiological importance. They are involved in electrical signaling in the heart and the nervous system, fluid secretions in the lung, gastrointestinal tract, kidney, and a variety of other key processes such as hormone secretions, the immune response, bone remodeling, and tumor cell proliferation [11,12]. Cellular functions in these organs require the passage of ions across the cell membrane. Because of this, drugs targeting ion channels can produce physiological changes in major body functions.

In excitable cells (nerve cells and various types of muscle cells), the orientation of the membrane potential is such that the cell interior is electrically negative against the outside at resting state. The orientation of the membrane potential is reversed for a brief period of time during excitation. This transient reversal is called the *action potential*. Its duration may vary from around 1 ms to several 100 ms depending on the cell type. This action potential rapidly spreads over the entire cell membrane, altering the functional state of the cell. Moreover, excitation of one cell often triggers excitation of neighboring cells by means of electrical or chemical coupling.

Ion channels are generally highly selective for the ions they conduct. More than 300 genes code for subunits of ion channels. Most ion channels can switch between

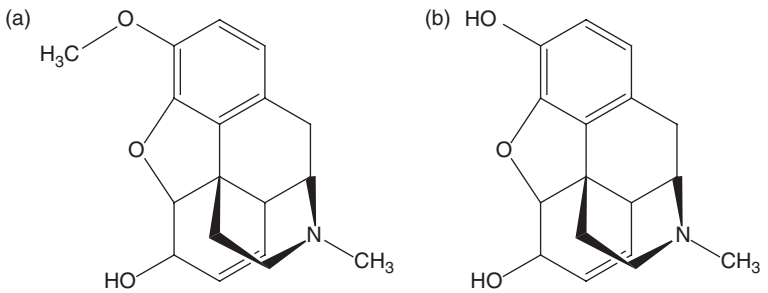

Figure 17.1 Structure of (a) codeine and (b) morphine. Structure determines interaction with the receptor.

open, closed, and inactivated states. Ion channels are classified by the principal ion they carry (sodium, Na^+; potassium, K^+; calcium, Ca^{2+}; and chloride, Cl^-) and the mechanism by which they are opened and closed. Ion channels can be categorized as follows:

1. *Ligand-Gated Channels.* These channels either open or close in response to ligand binding. For example, nicotinic acetylcholine receptors allow Na^+ ions into the cell in response to acetylcholine.
2. *Voltage-Gated Channels.* The conductance of these channels is regulated by changes in voltage across the plasma membrane. Local anesthetics block the conductance of Na^+ ions through voltage-gated sodium channels in neurons that transmit pain information from the periphery to the central nervous system and hence the pain perception.

Ion channels are multisubunit proteins, with each subunit predicted to span the plasma membrane multiple times. Symmetrical association of the subunits allows each to form a segment of the channel pore and to cooperatively control channel opening and closing. The ligand-binding domain can be extracellular, within the channel, or intracellular. Agonists may bind to a particular subunit that may be represented more than once in the assembled multimer (e.g., nicotinic acetylcholine receptor) or may be conferred to a single subunit of the assembled channel [e.g., sulfonylurea receptor that associates with the K^+ channels to regulate the ATP-dependent K^+ channels (K_{ATP})]. Sulfonylureas bind to the SUR1 subunits and block the ATP-sensitive potassium channels. Role of K_{ATP} in insulin release is shown in Fig. 17.2. Increase in blood glucose after a meal raises intracellular ATP concentration in the pancreatic β-cell and results in closure of K_{ATP} channels. It results in inhibition of potassium efflux and depolarization of the plasma membrane, thereby leading to increase in influx of calcium through voltage-sensitive calcium channels. Rise in $[Ca^{2+}]_i$ triggers exocytosis of insulin granules, thereby stimulating insulin secretion [13]. Openers of the same channel (K_{ATP}) may lead to membrane hyperpolarization, resulting in vascular smooth muscle relaxation (e.g., minoxidil).

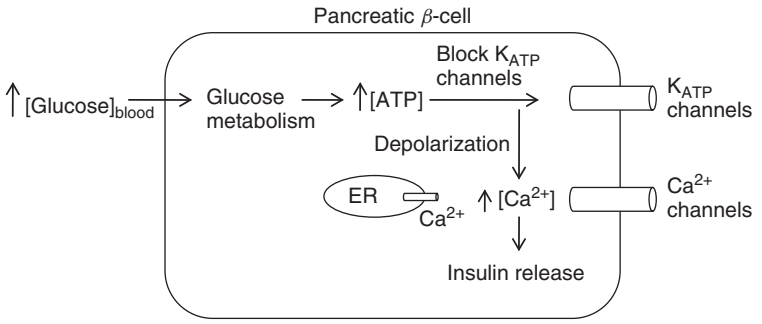

Figure 17.2 ATP-sensitive K^+ (K_{ATP}) channel as a major regulator of insulin secretion. *Source*: Adapted from Ref. 13.

17.2.2 G-Protein-Coupled Receptors

GPCRs are the target for more than 50% of the drugs currently in the market [14]. These proteins are expressed at the extracellular surface of the cell membrane, traverse the membrane, and possess intracellular regions that activate G-proteins. G-proteins are called so due to their interaction with the guanine nucleotides, guanosine triphosphate (GTP), and GDP. GPCRs bind to a wide variety of molecules, including biogenic amines, peptides, glycoproteins, lipids, nucleotides, ions, and proteases. They are involved in diverse biological functions, including the senses of smell, taste, and sight, and regulation of appetite, digestion, blood pressure, reproduction, inflammation, and so on [15,16]. GPCRs can be found in the central nervous system and in the periphery. Their role in different tissues may be different, although the second messengers that result from the initial activation are probably similar (e.g., muscarinic acetylcholine receptors, α- and β-adrenoceptors, serotonin receptors, and histaminergic receptors).

All GPCRs have seven transmembrane regions within a single polypeptide chain. In the resting state, G-proteins exist as attached αβγ trimer, with GDP occupying the site of the α-subunit. When the GPCR is occupied by an agonist molecule in the extracellular domain, a conformational change occurs and the G-protein binds to cytoplasmic domain of the receptor. Association of the αβγ trimer with the receptor causes the bound GDP to dissociate and to be replaced with GTP, which in turn causes dissociation of α-GTP unit from the βγ subunit. The α-GTP is the active from of the G-protein, which diffuses in the membrane and can interact with a number of different effectors. These effectors include adenylyl cyclase, phospholipase C, ion channels, and other classes of proteins. Signals mediated by G-proteins are terminated by the hydrolysis of GTP to GDP through the GTPase activity of the α-subunit. Different Gα-protein isoforms have now been identified, each of which have unique effects on their targets. A few of these G-proteins include G-stimulatory (Gs), G-inhibitory (Gi), Gq, G0, and G12/13. The major role of the G-protein is to activate the production of second messengers through different pathways. The key G-protein-coupled effector systems are briefly discussed below.

17.2.2.1 The Adenylate Cyclase/cAMP System. The cyclic 3′,5′-adenosine monophosphate (cAMP) is the nucleotide synthesized within the cell from ATP by the action of adenylate cyclase. It is produced continually and inactivated by hydrolysis to 5′-AMP by the action of phosphodiesterases. The cAMP in turn activates various protein kinases. These enzymes catalyze the phosphorylation of serine and threonine residues in different cellular proteins and thereby regulate cell function. The regulatory effects of cAMP on cellular function are diverse (e.g., energy metabolism, cell division, cell differentiation, ion transport, changes in neuronal excitability, and contraction of smooth muscles).

17.2.2.2 Phospholipase C/Inositol Phosphate System. Activation of phospholipase C, a membrane bound enzyme, hydrolyzes a membrane phospholipid, phosphatidylinositol-4,5-bisphosphate (PIP_2) to generate inositol-1,4,5-trisphosphate (IP_3) and diacylglycerol (DAG). IP_3 binds to receptors on Ca^{2+} channels in the endoplasmic reticulum, triggering the release of calcium. Calcium can bind to calmodulin and the resulting Ca^{2+}–calmodulin complex can further bind to intracellular enzymes such as Ca^{2+}-calmodulin-dependent protein kinases. Increase in intracellular Ca^{2+} is the major effector mechanism by which various neurotransmitters, hormones,

and drugs promote contraction of the smooth muscle. The other product, DAG, is hydrophobic, which remains associated with the membrane, activates protein kinase C, and controls phosphorylation of serine and threonine residues of a variety of intracellular proteins. Protein phosphorylation is the key mechanism through which many physiological mediators and drugs produce their effects. For example, release of hormones from many endocrine glands, increase or decrease in the neurotransmitter release and in neuronal excitability, and contraction or relaxation of smooth muscle. The role of GPCRs in regulating enzymes and ion channels is shown in Fig. 17.3.

The receptor-linked G-proteins can also activate phospholipase A2, which releases arachidonic acid and thus initiates synthesis of prostaglandins and related eicosanoid mediators. The receptor-linked G-proteins are involved in direct regulation of the ion channels. For example, muscarinic acetylcholine receptors are known to enhance K^+ permeability, thus hyperpolarizing the cells and inhibiting electrical activity.

17.2.3 Tyrosine Kinase and Guanylate-Cyclase-Linked Receptors

There are two classes of tyrosine kinases. Receptor tyrosine kinases (RTKs) are type I transmembrane proteins possessing an N-terminal extracellular domain, which can bind to an activating ligand, a single transmembrane domain, and a C-terminal cytoplasmic domain that includes the catalytic domain. Nonreceptor tyrosine kinases lack a transmembrane domain; most are soluble intracellular proteins and activated in a similar manner as RTKs.

The RTKs catalyze the transfer of phosphate from ATP to hydroxyl groups of tyrosine on target proteins. RTKs play an important role in the control of most fundamental cellular processes, including cell proliferation, cell cycle progression, metabolic homeostasis, transcriptional activation, neural transmission, and aging. They mediate signaling by insulin and a variety of growth factors such as epidermal growth factor (EGF), platelet-derived growth factor (PGF), and nerve growth factor. When activated, these receptors dimerize followed by autophosphorylation of tyrosine residues in the cytoplasmic domain. The phosphorylated tyrosine residues serve as the binding site for the SH2 domains of a variety of intracellular proteins, thereby

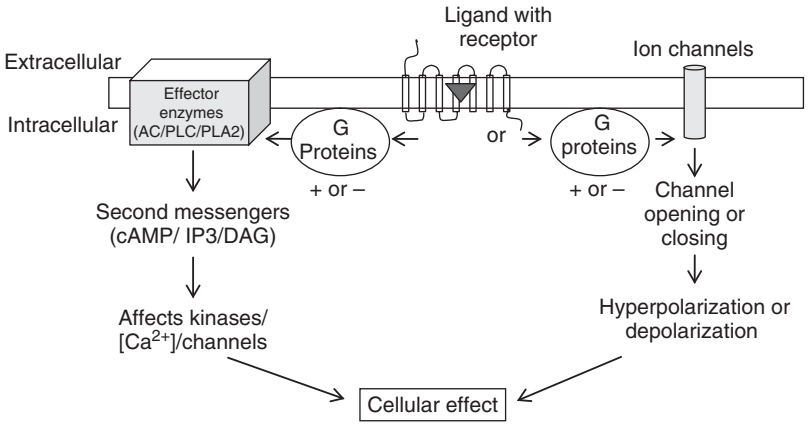

Figure 17.3 G-protein-coupled receptors and main signaling pathways. AC, adenylate cyclase; PLC, phospholipase C; PLA2, phospholipase A2; I, inositol triphosphate; DAG, diacylglycerol. *Source*: Adapted from Ref. 17.

allowing control of many cell functions. Important signaling pathways activated by RTKs include Ras/extracellular signal-regulated kinase mitogen-activated protein (ERK MAP) kinase cascade and PI-3 kinase pathway [18,19]. Examples of tyrosine kinase inhibitors approved recently are imatinib and dasatinib in chronic myeloid leukemia, gefitinib in lung cancer, and lapatinib in breast cancer.

Guanylate cyclase, a membrane bound enzyme, is similar in its regulation to the tyrosine kinase family. Receptors linked to guanylate cyclase, once activated lead to the production of 3′,5′-cyclic guanosine monophosphate (cGMP) from GTP. Natriuretic peptide, a hormone secreted from the ventricles in response to volume overload, acts via receptor guanylate cyclase.

17.2.4 Intracellular and Nuclear Receptors

Nuclear receptors that mediate the actions of classical hormones can be divided into two groups. Type I nuclear receptors include the steroid hormone receptors (e.g., androgen receptor, estrogen receptor (ER), glucocorticoid receptor, mineralocorticoid receptor, and progesterone receptor). When the receptor is not bound to a ligand, type I nuclear receptors are located in the cytoplasm associated with molecular chaperons (heat shock proteins) that maintain the receptors in a conformation that allows for ligand binding but not DNA binding. On hormone binding, type I nuclear receptors undergo a conformational change that results in the release of components of the chaperone complex, exposure of a nuclear localization sequence, and translocation to the nucleus where they associate with chromatin and regulate gene transcription [20].

The type II nuclear receptors include thyroid hormone receptor, vitamin D receptor, and retinoic acid receptor (RAR) and retinoid X receptor. In contrast to the type I nuclear receptors, the type II nuclear receptors reside in the nucleus, constitutively bound to DNA, and usually act as transcriptional repressors in the absence of hormone. Another class of nuclear receptors is called *orphan receptors*, for which regulatory ligands are still unknown (e.g., hepatocyte nuclear factor 4, HNF4α) [20]. Because of the essential role played by nuclear receptors in many aspects of mammalian development, metabolism, and physiology, dysfunction of signaling controlled by these receptors is associated with reproductive, proliferative, and metabolic diseases. For example, tamoxifen used in the treatment of breast cancer acts via ERα, retinoic acid used in acute promyelocytic leukemia acts via RARα receptors, and thiazolidinediones targeted in type II diabetes act via peroxisome proliferator-activated (PPARγ) receptors [21].

17.2.5 Desensitization or Tachyphylaxis

Desensitization or tachyphylaxis refers to a spontaneous decline in the response to a continuous or repeated application of agonist [7] and may be elucidated to prevent potential damage to the cell (e.g., high concentrations of calcium may initiate cell death). When repeated administration of a drug results in diminished response, the phenomenon is called *desensitization* or *tachyphylaxis*. This may develop in the course of a few minutes. The term *tolerance* is conventionally used to describe a more gradual decrease in response to a drug, taking days or weeks to develop. The desensitization of receptors may be due to change in receptor morphology, exhaustion of mediators, or loss of receptors (downregulation). Examples include morphine, ephedrine, and amphetamine.

17.2.6 Actions of Drugs Not Mediated by Receptors

Some drugs do not interact with macromolecular receptors to produce effect. For example, antacids such as sodium bicarbonate chemically neutralize gastric acid and reduce the symptoms of heart burn. Mannitol, an osmotic diuretic, is not reabsorbed in the renal tubule and increases the osmolarity of the glomerular filtrate, facilitating excretion of water. Cholestyramine resin, a lipid-lowering drug, sequesters bile acids in the intestine and decreases the absorption of exogenous cholesterol.

17.3 DRUG–RECEPTOR INTERACTIONS

17.3.1 Agonists

Ligands that bind to the receptor and alter the receptor state resulting in a biological response are called *agonists*. When bound by an agonist, a typical receptor is more likely to be in its active confirmation. Agonists may act by combining either with the same site as the endogenous agonist (primary or orthosteric site) or, less commonly, with a different region of the receptor macromolecule (allosteric or allotopic site). A full agonist has a strong affinity for its receptor and good efficacy. For example, phenylephrine is an agonist at α_1-adrenergic receptors. On binding to α_1-adrenoceptors on the vascular smooth muscle membranes, phenylephrine mobilizes intracellular calcium causing contraction of actin and myosin filaments, thereby decreasing the diameter of the blood vessel. Some agonists (e.g., glutamate) may only be effective in the presence of another ligand (e.g., glycine in the case of glutamate) that binds to a different site on the receptor. In such cases, glutamate is referred to as the *primary agonist* and glycine as a *coagonist* [7]. A typical relationship between response and agonist concentration is shown in Fig. 17.4.

As it can be seen in Fig. 17.4, the response increases with increase in agonist concentration. Up to a certain concentration, the response is directly proportional to the concentration, but at higher concentrations, the curve becomes asymptotic. This is the result of a capacity-limited, saturable process. To accommodate a wide range of concentrations, the relationship between effect and concentration is usually plotted on a semilog scale, which transforms the plot to a sigmoidal shape. When developing concentration–effect relationship, one may consider using free (not protein bound) drug

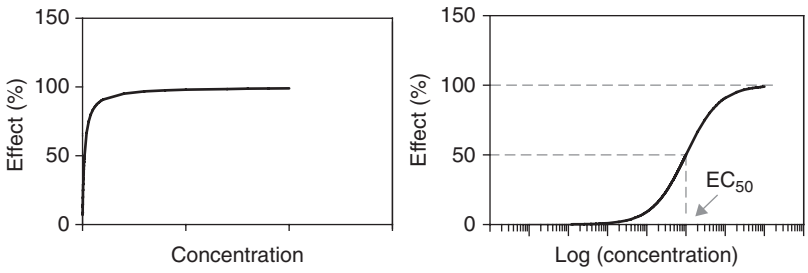

Figure 17.4 Concentration–effect relationship for an agonist.

concentrations since according to the free drug hypothesis, the free drug concentration at the site of action is the species that drives pharmacological activity.

17.3.2 Spare Receptors

Many agonists are able to produce maximal response without fully occupying all the receptors. Thus, not all the receptors in the tissue are required to achieve maximal response with some high efficacy agonists. Agonists may elicit the same maximal response, albeit at different receptor occupancies. This has been demonstrated experimentally by Furchgott (1966) and others that even with irreversible inactivation of some receptors, an agonist is still able to produce maximal response [7,22]. For example, at the skeletal neuromuscular junction, activation of $<1\%$ of receptors elicits an action potential and maximal contraction of muscle fibers. Hence, the neurotransmitter acetylcholine produces a maximum response by activating only a small proportion of receptors in the receptor pool.

17.3.3 Partial Agonists

A partial agonist cannot elicit as large an effect (even when applied at high concentrations to occupy all available receptors) as another agonist acting through the same receptors in the same tissue resulting in lower efficacy compared to full agonists (Fig. 17.5 [7]). Inability to produce a maximal response may be due to inability to convert the occupied receptors to an active form. For agents acting on opioid receptors, morphine and fentanyl are full agonists of the opioid receptors capable of inducing strong analgesia, while buprenorphine and pentazocine are partial agonists.

17.3.4 Inverse Agonists

Inverse agonists bind to receptors and reduce the fraction of receptors in active conformation [7]. This can occur when receptors exist both in active (R^*) and inactive

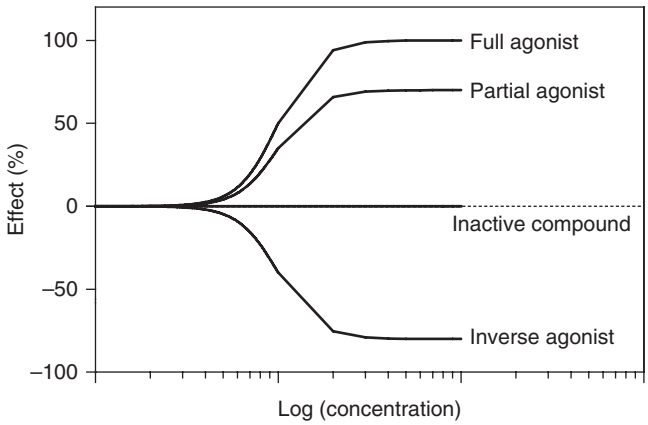

Figure 17.5 Different types of agonist action on receptors.

conformation in the absence of agonists:

$$\mathrm{R(inactive)} \Leftrightarrow \mathrm{R^*(active)}$$

An inverse agonist L, combines preferentially with inactive receptors, it will reduce the fraction in the active state:

$$\mathrm{LR\ (inactive)} \Leftrightarrow \mathrm{L + R\ (inactive)} \Leftrightarrow \mathrm{R^*(active)}$$

An inverse agonist may combine either with the same site as a conventional agonist or with a different site on the receptor macromolecule. Conventional agonists increase receptor activity, whereas inverse agonists reduce it. For example, antiallergic H_1 receptor antagonists, cetirizine, loratadine, and epinastine, may act through inverse agonism (i.e., stabilization of inactive confirmation of the histamine H_1 receptor) [23]. This has also been reported for several systems, including benzodiazepine and cannabinoid (CB) receptors.

17.3.5 Affinity

Affinity can be defined as the extent of binding to receptors at any given drug concentration. Drugs that have high affinity require fewer drug molecules to produce a certain degree of binding. However, affinity is not synonymous with efficacy, that is, an antagonist may have affinity but no efficacy. Affinity is usually represented as the reciprocal of the dissociation constant of the ligand–receptor complex (k_{-1}/k_1, where k_{-1} is the first-order rate constant of dissociation of ligand from the receptor and k_1 is the second-order rate constant of association of the ligand to the receptor). Refer to Section 17.6 for a schematic derivation of a receptor–ligand interaction.

17.3.6 Efficacy and Potency

Efficacy and potency can be determined by graded concentration–effect curves. The ability to produce a response is termed *efficacy* (intrinsic activity). Efficacy is a molecule-related property, and different molecules may have different capabilities to produce a physiological response. It is dependent on the number of drug–receptor complexes formed and the efficiency of subsequent transduction pathways. A drug with greater efficacy may be more therapeutically beneficial than one that is more potent (Fig. 17.6). Potency is an expression of the activity of a drug, in terms of the concentration or amount needed to produce a defined effect (e.g., EC_{50}). EC_{50} can be defined as the concentration of an agonist that produces 50% of its maximal possible effect. E_{max} is the maximal response produced by the drug. The agonist activities of drugs to induce a response can be categorized by comparing EC_{50} and E_{max}. The maximum response depends on efficacy. If an agonist has high efficacy, it does not necessarily mean that it will display high potency and vice versa.

17.3.7 Antagonist

A drug that reduces the action of another drug, generally an agonist, is referred to as *antagonist*. Antagonism may be competitive or noncompetitive. In competitive antagonism, the antagonist competes with the agonist for the binding site on the receptor.

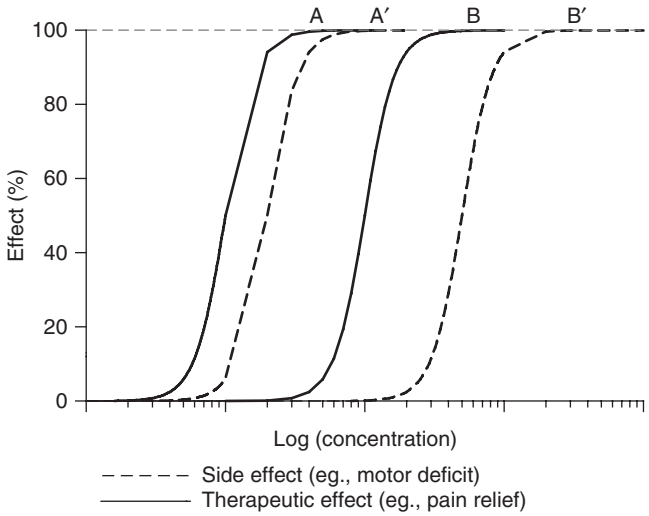

Figure 17.6 Concentration–effect relationship for two agents, A and B. A is more potent than B. A and B are equivalent in efficacy (e.g., pain relief). B is preferable than A due to its separation from concentration–effect relationship for side effect (e.g., motor deficit).

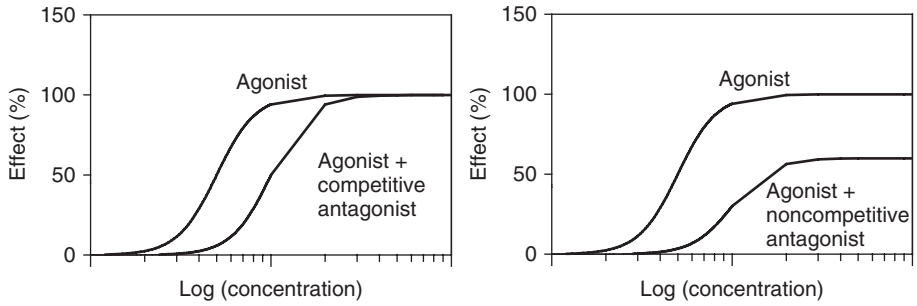

Figure 17.7 Effect of antagonist on agonist concentration–effect relationship.

For example, the antihypertensive drug prazocin competes with the endogenous ligand, norepinephrine at α_1-adrenergic receptors, thereby reducing blood pressure. Plotting the effect of the competitive antagonist shifts the agonist dose–response curve to the right. Noncompetitive antagonists can bind to either the active site or an allosteric site of the receptor. A characteristic difference between competitive and noncompetitive antagonists is that competitive antagonists reduce agonist potency, whereas noncompetitive antagonists reduce agonist efficacy (Fig. 17.7). For example, cyclothiazide is a noncompetitive antagonist of mGluR1 receptor (metabotropic glutamate receptors) by interacting at an allosteric site of the receptor [24]. In the case of physiological antagonism, the antagonist binds to a different receptor altogether. For example, histamine binds to H_1 receptors on bronchial smooth muscle, causing contraction and narrowing of bronchus, while epinephrine acts as an agonist at β_2-adrenoceptors on bronchial smooth muscle, causing relaxation.

In the following section, we have discussed how drug effects are measured at the molecular/physiological level. All these receptors, ion channels, and so on are part of systems such as organs. Efforts are being made recently to understand the progression of disease and drug effect on these systems. This understanding helps in identifying suitable entities in the system, which is more representative of the disease and hence more helpful in understanding the effect of a drug.

17.4 BIOMARKERS

The elucidation of the human genome and advances in proteome sciences have led to the identification of numerous potential novel pharmacological targets. Recent statistics in the drug discovery and development space, however, indicate that the failure rate of novel molecular entities (NMEs) is very high, with about 80% attrition occurring in clinical development [25]. The major factor responsible for this attrition is lack of efficacy and/or unacceptable safety. Most novel mechanisms turn out to be pharmacologically not viable as tested in proof-of-concept trials. Also, large epidemiological studies that characterize patient populations with respect to disease and its progression, as well as the role of pharmacologic targets in disease are lagging behind compared to the pace of new target identification at the molecular level. In order for drug discovery/development to be more successful, one needs to have the following:

1. increased probability of success of the unprecedented targets selected,
2. optimized validation of new targets,
3. selecting the best molecules, and
4. accelerating their advancement toward proof of concept in patients.

To stop prosecuting mechanisms or molecules that show insufficient early evidence of biological benefit is equally important, such that resources can be focused on more promising ones.

In a white paper published by the Food and Drug Administration (FDA) in 2004, titled "Innovation or Stagnation," the need for "a new product development toolkit" was emphasized. In order to improve the translation from laboratory concept to commercialized product, new powerful scientific and technological advances were recommended comprising *in silico* or animal models and biomarkers for safety, efficacy, and new clinical evaluation techniques. Ideally, biomarker research begins during the discovery phase, with strategic application during early clinical development and continued implementation through late stage development.

The Biomarkers Working Group (representation from the FDA, National Institute of Health (NIH), academia, and drug industry) arrived at a consensus definition of a biomarker as "a characteristic that is objectively measured and evaluated as an indicator of normal biological processes, pathogenic processes, or pharmacologic responses to a therapeutic intervention" [26]. Biomarkers may be of greatest value in early stages of the development of a drug to establish proof of concept in both *in vitro* and *in vivo* models.

A clinical end point is defined as a characteristic or variable that reflects how a patient feels, functions, or survives. Clinical end points reflect desired effects of

therapeutic intervention and are the most credible response measurements in clinical studies [26]. "A surrogate end point" is defined as a biomarker that is intended to substitute for a clinical end point. A surrogate is expected to predict clinical benefit (or harm or lack of benefit) based on epidemiologic, therapeutic, pathophysiologic, or other scientific evidence [26]. The actual clinical outcome has been classically measured as morbidity/mortality parameters or how a patient is functioning and feeling. Relatively few biomarkers have qualified for the evidentiary status of a surrogate end point. The availability of predictive biomarkers is a key factor in translational approaches in drug discovery and development. Their strategic application has utility at several stages, for example,

- demonstrate proof of target engagement in nonclinical species,
- facilitate design and/or selection of lead compounds,
- predict toxicity in nonclinical species,
- selection of first-in-human (FIH) dose,
- design of early clinical trial,
- enable go-no-go decisions toward expensive late phase trials,
- choice of appropriate patient populations,
- demonstrate proof of concept in disease in humans,
- estimation of therapeutic index, and
- regulatory approvals based on surrogate clinical end points.

17.4.1 Types of Biomarkers

17.4.1.1 Proximal and Distal Biomarkers. Biomarkers employed during early clinical development serve to demonstrate target engagement and are termed as *proximal biomarkers*. They inform on the concentration–response relationship between drug PK and modulation of a selected pharmacological response, such as receptor occupancy, *ex vivo* inhibition of an inflammatory marker, kinase inhibition, change in mRNA, and target enzyme activity. Selected examples of proximal biomarkers used in proof-of-pharmacology assessment of novel entities are listed in Table 17.1 [27].

Disease-related biomarkers, termed as *distal biomarkers*, are employed at the same time or somewhat later in the clinical development to demonstrate effect of target modulation by the drug on disease pathophysiology. These biomarkers assess drug's effect on a disease, are linked to clinical benefits, and thus have the potential of qualifying as surrogate end points. Examples are blood pressure reduction, insulin and blood glucose modulation, cholesterol and HDL modulation, and ACR20 score in rheumatoid arthritis. For additional examples, refer to Table 17.1 [27].

17.4.1.2 Technology-Based Classification of Biomarkers. Depending on the biological target and therapeutic area, a variety of pathway- or disease-related biomarkers have been proposed. Roughly, they can be classified as "-omics"-based (genomic, proteomic, and metabolomic), activity-based, or imaging-based approaches.

TABLE 17.1 Proximal and Distal Biomarkers in Different Disease Areas

Therapeutic Area	Proximal Biomarker	Distal Biomarker	Examples	References
Diabetes	Dipeptidyl peptidase-4 (DPP-4) Glucagon-like peptide-1 (GLP-1) Adiponectin Urinary glucose excretion	Blood glucose HbA1c	Sitagliptin, PPAR agonists, Dapagliflozin	27,35,36
Obesity	Positron emission tomography for targets NYP-5 and CB-1	Body weight	MK-0557 MK-9470	27,37
Cardiovascular: Hypertension and Atherosclerosis	C-reactive protein, HDL, LDL, adiponectin, Serum thromboxane B_2 levels, Plasma renin activity	Blood pressure	Statins, Aspirin, BAY-10-6734	38–40
Immunology: Rheumatoid arthritis	Tumor necrosis factor α (TNF-α), Multiple cytokines, MCP-1-induced chemotaxis in synovial fluid	ACR20 score	Infliximab	41
Alzheimer's disease	β-Amyloid peptide in CSF and plasma	Cognitive score	LY450139	42
Multiple sclerosis	Lymphocyte count	Aggregate relapse rate and physical disability	Fingolimod	43

17.4.1.2.1 "-omics"-Based Biomarkers. Genomics provides a measure of the transcribed genome (transcriptome). Pharmacogenomics has evolved as one of the main applications of biomarker discovery and has delivered decision-making biomarkers. Examples are provided in Table 17.2. Translatability has been achieved by profiling effects of drug treatment on gene expression in cell/tissue culture or *in vivo* in animals and clustering certain genes/pathways for further validation in human trials. Standardization of gene expression microarrays or gene chip technologies has had a tremendous impact in facilitating the use of this approach in biomarker discovery and development. Genomics is different from genetics in that the latter is an analysis of genome in normal

TABLE 17.2 Examples of Genomic Biomarkers

Drug	Indication	Biomarker
Imatinib mesylate	Stomach cancer	C-KIT expression
Boceprevir	Hepatitis C virus	il28B
Cetuximab	Colorectal cancer	EGFR expression
Cetuximab	Colorectal cancer	KRAS
Maraviroc	HIV	CCR5
Trastuzumab	Breast cancer	Her2/neu expression
Irinotecan	Colon rectum cancer	UGT1A1 variant

or disease state, including identification of genetic variants (insertion, deletion, amplification, single nucleotide polymorphisms, etc.). The correlation of genetic variation in disease state has the potential to provide mechanisms of drug action and select appropriate patient population. One of the earliest examples was the enrollment of breast cancer patients positive for HER2 amplification for treatment with trastuzumab [28]. Another genomic application for patient selection/labeling is that of polymorphic drug metabolizing enzymes CYP2D6, CYP2C9, and CYP2C19. Depending on the CYP allele, patients may be extensive or poor metabolizers of drugs that are primarily metabolized by these enzymes, potentially leading to a significant variability in drug exposure. The US FDA Web site provides a table of pharmacogenomic biomarkers in drug labels and is available at www.fda.gov/drugs/scienceresearch/researchareas/pharmacogenetics. There is increasing evidence that pharmacogenomics can play an important role in identifying responders and nonresponders to medications, avoiding adverse events, and optimizing drug dose. Drug labels containing information on genomic biomarkers describe the following:

- drug exposure and clinical response variability,
- risk for adverse events,
- genotype-dependent dosing,
- mechanisms of drug action, and
- polymorphic target and disposition genes.

Using gene expression arrays (e.g., Affymetrix) as PD biomarkers has certain limitations [29]. In a rat model of rheumatoid arthritis, methylprednisolone was administered exogenously to normal and diseased rats and cytokine gene expression changes were monitored. Normal rats were shown to exhibit circadian rhythms in gene expression in the liver and muscle that peaked at a time different from the disease rats. After a single dose of methylprednisolone, the gene expression may show a biphasic response and the change in gene expression may not be predictive of that after chronic administration.

Consistency in gene expression across different laboratories is also a challenging issue, so is the influence of environmental factors. Owing to the complexity and variability of gene expression profiles, combination with other biomarkers is often necessary.

Proteomics may be considered a more direct approach to the discovery of mechanistic/functional biomarkers of drug action. The proteome is more complex than the genome and transcriptome and reflects protein abundance, posttranslational modifications, localization in cells, and interaction with other macromolecules. Although this complexity defines the biological homeostasis, it also makes it difficult to identify protein biomarkers and establish robust/reproducible assays that quantify drug-related changes. Defined panels of candidate protein biomarkers can be analyzed via high throughput technologies, such as protein arrays and multiple-reaction monitoring mass spectrometry. ELISA-based protein immunoassays are still considered the gold standard. In Alzheimer's disease, the levels of disease-related CSF biomarkers such as amyloid β-peptide 1-42 (Ab42), tau, and phosphorylated tau (p-tau) may increase diagnostic accuracy. Good correlation is observed in the levels of CSF biomarkers and amyloid imaging by PET.

Metabolomics encompasses the effect of drug treatment on small-molecule endogenous biochemicals, as a result of activation or inhibition of their biosynthentic and/or

disposition pathways. Many of these biomarkers form a part of standard clinical chemistry panels and are applied in the detection of organ-based toxicity. Glucose and cholesterol are examples of metabolomic biomarkers that have been successfully applied in the development and approval of antidiabetic and antiatherosclerotic therapies, respectively. Together, the genetic, genomic, proteomic, and metabolomic approaches constitute "molecular profiling."

17.4.1.2.2 Activity-Based Biomarkers. Pharmacological target-based activity assays represent the most direct assessment of functional activity of new drugs. Given that plasma remains the most accessible biological fluid during clinical development, *ex vivo* whole-blood or plasma biomarkers are highly desirable. *Ex vivo* whole-blood CD11b, tumor necrosis factor α (TNF-α), or suitable interleukin (IL) assays as inflammatory biomarkers (Table 17.1). Depending on drug distribution, and anticipated site of action, tissue fluids such as CSF and synovial fluid are sampled or tissue biopsies such as liver or tumor are accessed for analysis of biomarkers.

17.4.1.2.3 Imaging-Based Biomarkers. Molecular imaging refers to noninvasive or minimally invasive technologies for visualizing, characterizing, and quantifying anatomical structures and physiological processes at the cellular and subcellular levels, with exquisite spatial, temporal, and biochemical resolution *in situ* and *in vivo* [30]. PET, single photon emission computed tomography (SPECT), computer tomography (CT), magnetic resonance imaging (MRI), ultrasound (US), and optical imaging are used for biomarker measurement. These techniques differ in terms of the mechanisms used to generate images, imaging probe characteristics, and their resolution and sensitivity. The most commonly used imaging approach is nuclear imaging that visualizes radiotracers interacting with protein targets located intracellularly or on the cell surface. PET uses ^{11}C and ^{18}F, while SPECT uses ^{123}I as radionuclides. They are used for tracking the drug itself (small molecule or protein), imaging the pharmacological target, or monitoring key biochemical and physiological processes. There are a few examples in which imaging techniques have been used to support drug registration (oncology, neurology, cardiovascular, and musculoskeletal). There are other examples in which these techniques have been used to make early go-no-go decisions, in the CNS and obesity area from Merck laboratories: for example, CB-1 receptor inverse agonist MK-9470 and neuropeptide receptor Y5 (NPY5) receptor antagonist MK-0557 [27].

In order to select appropriate biomarkers and incorporate them into the design of clinical trials, it is important to be aware of the wide variation in the turnover rates of biomarkers. For example, electrical signals, neurotransmitters, and chemical signals turn over in seconds; hormones, enzymes, and mRNA in several hours; cells and tissues in weeks; organs such as bone in 10 years; and human life span in 100 years.

17.4.2 Biomarker in Different Stages of Drug Development

In early research, the selection of biomarkers to support mechanistic studies in cell-based and animal models should depend on their translation to human samples. Biomarkers to investigate target engagement and its efficacy on disease status should be incorporated in early clinical trials, as it helps assess the possibility of success

in large-scale clinical trials by relating clinical data to preclinical test systems and by determining whether drug is affecting the molecular target and whether it is translating into therapeutic benefit. The use of biomarkers in clinical development can be categorized into four types and show increasing decision-making and regulatory application:

1. *Exploratory.* Supported by *in vitro* and preclinical data but with no consistent information regarding their link to clinical outcome in humans.
2. *Demonstrated (Probable Valid).* With sufficient preclinical sensitivity and specificity and are linked to a clinical outcome but without reproducible evidence.
3. *Characterized.* Both preclinical and clinical validation, as listed in "1" and "2" above, as well as show reproducibility in more than one prospective clinical study.
4. *Surrogate.* Biomarkers that demonstrate utility as a substitute for a clinical end point. This scheme shows the increasing decision-making and regulatory application.

Biomarker qualification represents the progressive transition from exploratory stage to surrogacy. Biomarkers may also enter qualification stage from general medical practice. For example, low density lipoprotein (LDL) cholesterol was in general medical use before its role in drug development. Biomarkers may also be "disqualified" if evidence does not support their intended use. For example, suppression of intermittent ventricular tachyarrhythmia as a marker of reduction in ventricular arrhythmia and mortality due to myocardial infarction was disqualified as a biomarker because a controlled cardiac arrhythmia suppression trial demonstrated that mortality was increased by antiarrhythmic treatment following an infarction.

The process of biomarker qualification gauges the evidentiary status from exploratory application to prediction of clinical outcome. A consensual framework is required to define surrogacy due to the current lack of consistent evidentiary standards, as identified in FDA's critical path initiative. Lathia *et al*. [31] have reviewed the types of evidence supporting or not supporting certain surrogate end points. A complication in selecting "a" surrogate end point is that most outcomes are multidimensional, thus crucial information such as safety issues can be missed by employing a single measure. Thus, based on preclinical information, it is better to use multiple biomarkers to evaluate efficacy and safety during development of drug candidates. FDA-NIH consensus conference on biomarkers (1999), FDA Critical Path Initiative (2004) [32], and European Medical Agency Roadmap (EMEA, 2010) [33] have advocated different biomarker strategies. The biomarker consortium, a public–private collaboration was launched in 2006. The role of consortia (among regulatory, industrial, academic, and government representatives) in biomarker development and application enables collaborative pooling of (precompetitive) data and benefits all participants by increasing the availability of validated and qualified biomarkers. In order to promote qualification and regulatory acceptance of biomarkers, research data and results are made broadly available to public to help speed disease-specific research.

Successful application of PK-PD modeling in drug discovery and development depends on a thorough understanding of the following:

1. the disposition of the molecular entity being developed, including its Absorption, Distribution, Metabolism, Excretion (ADME) characteristics in preclinical species and human;
2. the pharmacology of target modulation, including assessment of potency and efficacy in *in vitro* binding and functional assays and *in vivo* concentration–response relationships in preclinical species and human; and
3. the disease pathophysiology, including a cause–effect relation between the target and disease and effect of drug on disease or surrogate end points

Therefore, biomarkers play a major role in discovery of target, evaluation of drug candidates in preclinical models, early- and late-phase clinical development, and approval from federal agency with the help of PK-PD modeling incorporated in clinical trial simulations, as exemplified in a recent Pfizer article by Morgan *et al*. [34].

17.5 MATHEMATICAL MODELS IN PHARMACODYNAMICS

PK-PD modeling has been gaining its importance in both drug discovery and development stage in recent years. In one of their reports in 2004, Donald Stanski, the scientific advisor to the Center for Drug Evaluation and Research, FDA, stated that "the latest buzzwords at the FDA are model-based drug development" [44]. The primary objective of PK-PD modeling is to characterize drug-specific parameters such as $E_{\max}$ and EC_{50}, as defined in Section 17.2, as well as system-specific factors such as production (k_{in}) and dissipation (k_{out}) rates of PD responses, k_{e0}, tau (τ), as has been defined in this section. The effect of a drug that depends on its interaction with the receptor is usually known as *primary effect*. The primary effect causes the physiological system and its various components to respond, which translates to clinical response [45]. In preclinical studies, PK-PD modeling is often used to estimate the FIH dose. Another application is the use of physiological modeling and allometry of PK/toxicokinetic data and extrapolation of the results from animals to human. In clinical settings, PK-PD modeling is used to interpret the dose–response data for single ascending dose (SAD) studies and decide doses for the dose escalation studies. This is primarily true where a single dose exhibits change in the PD biomarker. PK-PD modeling also has been used by the FDA to propose dose or dosage regimen(s) that were not originally recommended by the sponsors. A variety of mathematical models have been used to analyze different types of PD responses. There are two kinds of response. A graded or continuous response is a one where the response can be measured as a continuous function of dose, concentration, or time. These types of data have been typically modeled by deterministic models. Examples of such response data would be change in heart rate, temperature, and enzyme activity. The other type of response is known as *dichotomous response* and is either "all" or "none." Stochastic models have been used to analyze this kind of data. In this section, we describe the different types of models typically used to describe dose–response or exposure–response data and encompass the basic model structure, PK-PD expectations from these types of models, determination of initial estimates of drug-specific and system parameters, and applications reported in

the literature. Additional complexities outside the scope of this discussion provided can be found in the References section.

17.6 CONCENTRATION–RESPONSE RELATIONSHIP

A drug must bind to its target in order to exert its PD effects. As discussed previously, these proteins may be enzymes, transporters, ion channels, or receptors. The most popular and appropriate model for receptor occupancy, proposed by Clark, is based on law of mass action. The law of mass action and small quantity of receptors lead to capacity limitation for most responses (Jusko WJ, State University of New York at Buffalo, New York, personal communication, March 2006). Below is a schematic representation of drug–receptor interaction:

$$[\mathrm{C}] + [\mathrm{R}] \leftrightarrow [\mathrm{R} - \mathrm{C}]$$

Let us suppose that [C] is the concentration of drug at the site of action, [R] is the available concentration of receptors, RTOT is total concentration of receptors (bound+free), and RC is the concentration of the drug–receptor complex. The primary assumption is that the effect is proportional to the drug–receptor concentration at a given time. At equilibrium, the rate of formation of the drug–receptor complex, governed by a second-order rate constant k_1 is equal to the rate of dissociation of the RC complex, governed by the first-order rate constant k_{-1}. Thus, the equation for the drug–receptor complex is as follows:

$$\frac{\mathrm{d}[\mathrm{RC}]}{\mathrm{d}t} = k_1 \cdot [\mathrm{R}] \cdot [\mathrm{C}] - k_{-1} \cdot [\mathrm{RC}] \tag{17.1}$$

At equilibrium when

$$\frac{\mathrm{d}[\mathrm{RC}]}{\mathrm{d}t} = 0 \tag{17.2}$$

$$k_1 \cdot [\mathrm{R}] \cdot [\mathrm{C}] = k_{-1} \cdot [\mathrm{RC}] \tag{17.3}$$

$$\frac{[\mathrm{R}] \cdot [\mathrm{C}]}{[\mathrm{RC}]} = \frac{k_{-1}}{k_1} = K_\mathrm{D} \tag{17.4}$$

where K_D is the equilibrium dissociation constant. A lower value of K_D indicates a poor dissociation of the drug–receptor complex translating into high affinity of the drug for a given receptor.

Solving for [RC] yields

$$\frac{([\mathrm{R_{Tot}}] - [\mathrm{RC}]) \cdot [\mathrm{C}]}{[\mathrm{RC}]} = \frac{k_{-1}}{k_1} = K_\mathrm{D} \tag{17.5}$$

Rearranging the above equation, one can arrive at

$$\frac{[\mathrm{RC}]}{[\mathrm{R_{Tot}}]} = \frac{[\mathrm{C}]}{[\mathrm{C}] + K_\mathrm{D}} \tag{17.6}$$

Ariens [46] introduced the concept that effect is directly proportional to the concentration of the drug–receptor complex and the proportionality constant ε was called the *intrinsic activity of the agent*:

$$\varepsilon = \frac{[\mathrm{RC}]}{E} \tag{17.7}$$

The maximal drug response occurs when all the receptors are occupied and thus,

$$\varepsilon = \frac{[\mathrm{R_{Tot}}]}{E_{\max}} \tag{17.8}$$

Substituting in Equation 17.6 yields the following equation:

$$E = \frac{E_{\max} \cdot [\mathrm{C}]}{[\mathrm{C}] + K_{\mathrm{D}}} \tag{17.9}$$

K_{D}, the affinity for the drug can be replaced by EC_{50} (or the potency) for the agent to yield Equation 17.10. EC_{50} is defined as the concentration of the drug that produces 50% of its maximum effect:

$$E = \frac{E_{\max} \cdot [\mathrm{C}]}{\mathrm{EC}_{50} + [\mathrm{C}]} \tag{17.10}$$

Thus, the binding of a drug to the receptor can translate to the clinical response E. In PD modeling, a drug bound to a receptor may either stimulate (S) or inhibit (I) a process as described by the following equations:

$$S = 1 + \frac{S_{\max} \cdot [\mathrm{C}]}{\mathrm{SC}_{50} + [\mathrm{C}]} \tag{17.11}$$

$$I = 1 + \frac{I_{\max} \cdot [\mathrm{C}]}{\mathrm{IC}_{50} + [\mathrm{C}]} \tag{17.12}$$

17.7 CLASSIFICATION OF MATHEMATICAL MODELS IN PHARMACODYNAMICS

Figure 17.8 depicts the classification of different types of models used to analyze PD data. The models have been described in details in the following sections.

17.7.1 Reversible Effect Models

This category refers to the type of responses that return to the baseline or predose (physiological) levels as the drug is eliminated from the system (e.g., inhibition or stimulation of synthesis or dissipation of response, cell trafficking, and enzyme induction), causing no permanent damage to the system.

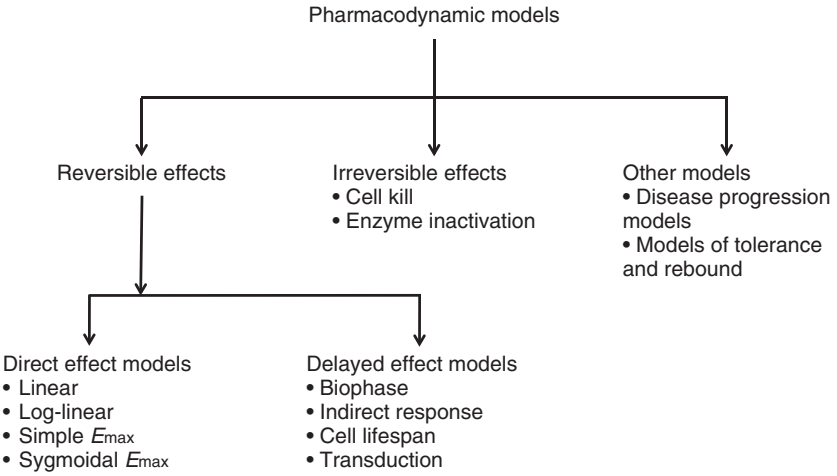

Figure 17.8 Types of pharmacodynamic models.

17.7.1.1 Direct Effect Models. A direct effect is observed when the action of the drug on its target is so rapid that there is no delay observed between the PK and PD profiles, for example, vascular targets or very rapid turnover processes such as muscle activity. The basic expectation of these effects is depicted in Fig. 17.9a and b. Figure 17.9a represents PK (C vs t) and Fig. 17.9b depicts effects versus time. Equation 17.13 represents the PK and Equation 17.14 represents the PD:

$$C_{\mathrm{P}} = \frac{D}{V} \cdot \mathrm{e}^{-k_{\mathrm{el}} \cdot t} \tag{17.13}$$

$$E = \frac{E_{\max} \cdot C}{\mathrm{EC}_{50} + C} \tag{17.14}$$

At $C_{\max}$, the effect reaches a maximum of 100. As the drug is eliminated, the effect diminishes and reaches a minimum at a sufficiently low drug concentration.

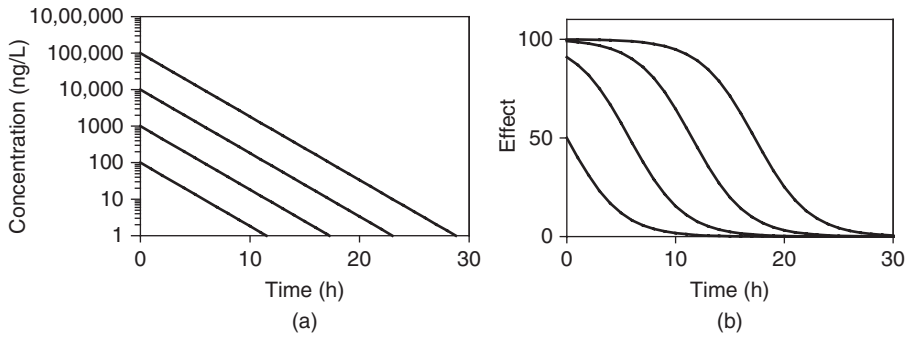

Figure 17.9 PK/PD expectations in case of direct effects. (a) Monoexponential PK and (b) PD. $k_{\mathrm{el}} = 0.4$ units, $V = 10$ units, $E_{\max} = 100$, $\mathrm{EC}_{50} = 100$.

17.7.1.1.1 Linear Effect Concentration Model. The simplest relationship between effect and concentration is represented by the following equation:

$$E = m \cdot C \tag{17.15}$$

This equation indicates that effect is zero when there is no drug present in the body and it increases with slope "*m*" as the concentration of the drug in the body increases. A situation very similar to this could be the presence of baseline of effect (E_0), which is represented by Equation 17.16. At $C = 0$, the effect is E_0. As the concentration increases, the effect increases linearly with a slope "*m*." "*m*" can be easily estimated from the slope of the effect versus concentration plot:

$$E = E_0 + m \cdot C \tag{17.16}$$

17.7.1.1.2 Log-Linear Effect Concentration Model. This model finds its application in cases where the concentration varies over a wide range and appears curvilinear when plotted without log transformation. On log transformation, the data appear linear and the slope "*m*" can be estimated easily as described above (Eq. 17.17). The main assumption of this model is that changes in drug concentration and effect are proportional to one another:

$$E = m \cdot \log C + E_0 \tag{17.17}$$

17.7.1.1.3 Simple and Sigmoid E_{max} Models. A simple E_{max} and sigmoid E_{max} model is depicted by Equations 17.18 and 17.19, respectively:

$$E = \frac{E_{max} \cdot C}{EC_{50} + C} \tag{17.18}$$

$$E = \frac{E_{max} \cdot C^{\gamma}}{EC_{50}^{\gamma} + C^{\gamma}} \tag{17.19}$$

E_{max} indicates the maximum response caused by the drug. EC_{50} is defined as the concentration of the drug, which produces half the maximal response. The PK-PD expectation is shown in Fig. 17.9. In sigmoid E_{max} model, a shape factor is added to the simple E_{max} to make the slope of the response steeper or shallower. Figure 17.10 depicts how the values for the shape factor, γ, affect the profile. This shape factor provides more flexibility to the function so that the function can orient itself according to the shape of the data.

17.7.1.2 Delayed Effect Models. A drug, after administration, may produce effects which may be delayed from the PK. The maximum effect does not occur at the same time as the maximum plasma concentration. This may be due to distributional delays, turnover of endogenous proteins, or signal transduction. In this type of data if the plasma concentrations from each time point are plotted with the effect at the corresponding time point, they do not produce a hyperbolic profile but produce hysteresis (Greek meaning, the state of being behind or late). Figure 17.11a shows a typical PK-PD expectation for a delayed effect. The PK profile peaks at 1 h and the response peaks

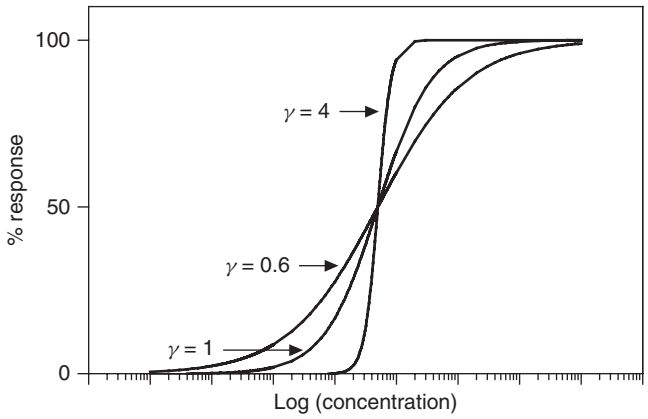

Figure 17.10 Effect of the values of γ on the profiles of a simple E_{max} model.

at 2 h. Thus, the PD response in delayed by 1 h. Figure 17.11b shows a prototypical hysteresis plot produced when concentration is plotted against effect in case of delayed effects. For the same concentration of 40 units, there are two effects, 95 and 105 units. This profile cannot be analyzed using simple E_{max}-type model to resolve estimates of drug efficacy/potency. To obtain accurate estimates of efficacy, the PK-PD model needs to incorporate a component that captures the delay. In this section, we have made an effort to identify different types of mechanistic and empirical approaches, which account for these delays in drug response.

17.7.1.2.1 Biophase Model or Link Model. Biophase or link model has been applied to data where drug distribution to the site of action is assumed to be the rate-limiting factor for effect to occur. The term *biophase* was first coined by Furchgott [47]. This modeling approach was proposed and popularized by Sheiner *et al*. [48] for drugs showing delay in response. In their publication, Sheiner *et al*. included a hypothetical delay compartment to account for the disconnection observed in the PK and PD of the compound.

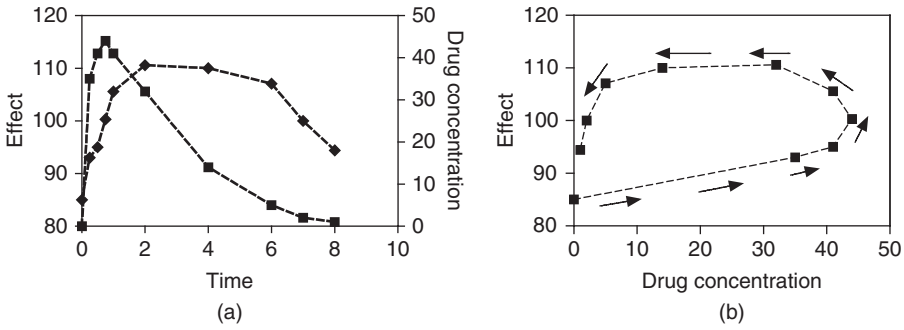

Figure 17.11 (a) Typical PK-PD expectation for a delayed PD effect and (b) hysteresis after plotting concentration with effect.

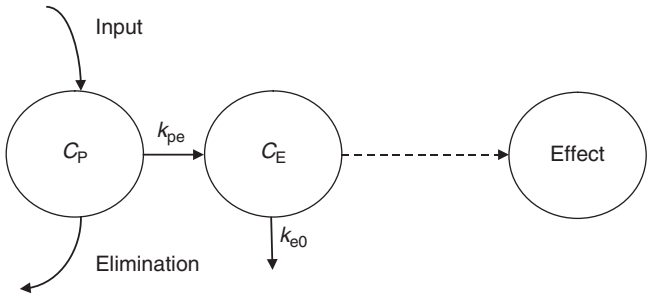

Figure 17.12 Biophase/link model.

The structure of the model is depicted in Fig. 17.12. C_P is the concentration of drug in plasma and C_e is the concentration of drug in the hypothetical effect compartment. Drug enters plasma by "input" and is eliminated by "elimination." It also distributes to a hypothetical effect compartment by the rate constant k_{pe} and this distribution causes the delay for the observed effect. The basic assumption of this model is that the hypothetical effect compartment does not alter the PK of the drug. The plasma PK parameters are fixed. The rate constants k_{pe} and k_{e0} are assumed to be the same (k_{e0}) due to lack of identifiability. Thus, k_{e0} is defined as the rate constant causing distribution of drug to the hypothetical effect compartment and thus causing delay. An E_{max} model is then used to describe the effect versus time profile and C_p in the E_{max} equation is replaced by C_e, as shown in the following equations:

$$\frac{dC_e}{dt} = k_{e0} \cdot C_P - k_{e0} \cdot C_e \tag{17.20}$$

$$E = \frac{E_{max} \cdot C_e}{EC_{50} + C_e} \tag{17.21}$$

The biophase/link model has been widely used in the literature to model PK-PD relationship of drugs showing delays in effect [49–51]. A nice example of using a biophase model to account for delay of electroencephalography (EEC) effect by midazolam, when using arterial sampling, was demonstrated by Tuk *et al*. [52]. Arterial data showed anticlockwise hysteresis but no hysteresis was observed with the use of venous concentrations.

SIGNATURE PROFILES. Figure 17.13 shows the simulations performed on a typical biophase or link model. The following parameter values were used to perform the simulations:

$$k_{el} = 0.4,\ k_{e0} = 0.5,\ E_{max} = 100,\ EC_{50} = 100,\ V = 1,\ \text{dose} : 10, 100, 1000, 10{,}000 \text{ units}$$

As one would expect, the peak effect occurs at a later time than that of C_{max}. T_{max} of the effect is the same for all doses. Decreases in values of k_{e0} will produce more delay. On the basis of the values of k_{e0}, the effect compartment may produce flip-flop kinetics.

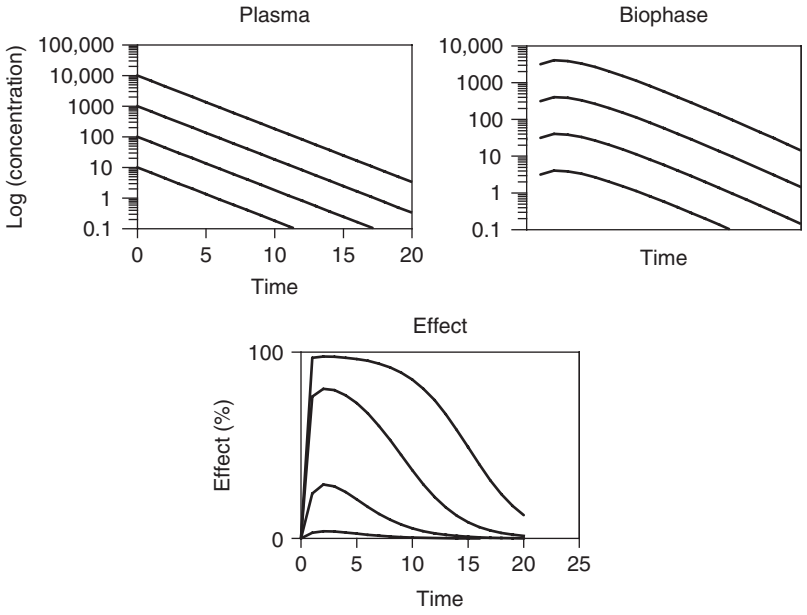

Figure 17.13 Signature profiles of plasma compartment, effect compartment, and response versus time profiles for a biophase model. $k_{el} = 0.4$, $k_{e0} = 0.5$, $E_{max} = 100$, $EC_{50} = 100$, $V = 1$, dose: 10, 100, 1000, and 10,000 units.

EFFECT OF k_{e0} ON SIGNATURE PROFILES. Figure 17.14 depicts the effects of changing k_{e0} on the signature profiles of a biophase model. The dotted line is the plasma concentration and the solid lines depict biophase concentrations at different values of k_{e0}. The value of the elimination rate constant, k_{el} is 0.4 and three profiles of biophase concentrations for k_{e0} values of 0.1, 0.4, and 1 have been plotted. When k_{e0} and k_{el}

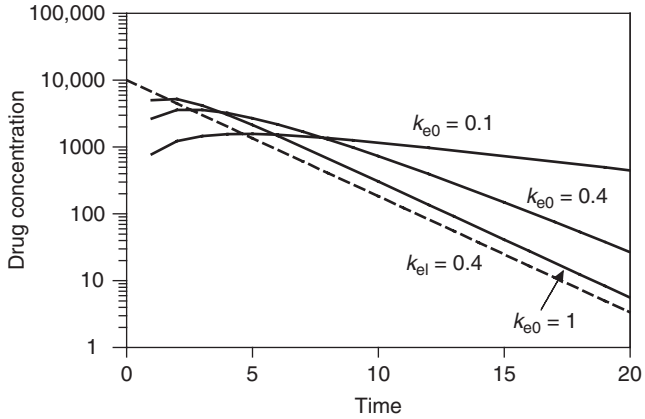

Figure 17.14 Effect of different values of k_{e0} on shapes of hypothetical effect compartment. $k_{e0} = 0.1$, 0.4, and 1. $k_{el} = 0.4$. Dotted line, central compartment; solid lines, hypothetical effect compartment.

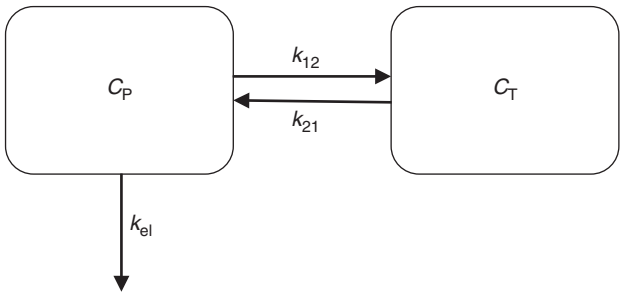

Figure 17.15 Schematic diagram of a mammillary two-compartment model.

are equal ($k_{e0} = k_{el} = 0.4$), the biophase and plasma profiles are not exactly parallel and the biophase profile seems curvilinear. In this case the explicit solution for the biophase compartment is slightly different and is outside the scope of this chapter. The terminal phase of the biophase concentrations is parallel to the plasma concentrations when value of k_{e0} is 1. When k_{e0} is 0.1, the terminal phase of the plasma concentrations and biophase concentrations are not parallel. Thus, this model has a flexibility of capturing PK-PD data where drug leaves the body but the effect still prevails, with values of k_{e0} less than the terminal phase of the PK profile.

DIFFERENCE WITH A MAMMILLARY TWO-COMPARTMENT MODEL. Figure 17.15 depicts a mammillary two-compartment PK model. C_P represents drug concentrations in the central (plasma) compartment and C_T represents drug concentrations in some hypothetical tissue compartment where the drug can distribute to. The first-order rate constant k_{el} represents the elimination rate constant for drug from the central compartment, and k_{12} and k_{21} are first-order rate constants representing distribution from plasma to tissue and tissue to plasma, respectively. Drug is eliminated only from the central compartment. Primarily, there are three disadvantages of using a two-compartment model instead of a biophase model. First, the number of parameters is one more than a biophase model since one has to use k_{12} and k_{21} instead of just k_{e0}. Second, if the plasma kinetics of the drug in monophasic, adding a tissue compartment will always make the plasma concentrations biphasic. In other words, a tissue compartment affects the concentrations of the plasma compartment. But the assumption of a biophase model is that the effect compartment does not alter the plasma concentrations. Third, no matter what value we use for k_{12} and k_{21}, the tissue concentrations will always decline parallel to the plasma concentrations for a two-compartment mammillary model. Whereas for a biophase model, the effect site concentrations do not decline parallel to the plasma concentrations for k_{e0} values less than the elimination rate constant.

INITIAL ESTIMATES. Figure 17.16 describes the method for estimation of k_{e0}. The rationale for taking the difference between time of peak effect and time of peak plasma concentration arises from the belief that the delay observed in effect is due to distribution of the drug to the effect compartment or biophase. If one had biophase concentrations, the time of peak biophase concentrations would be the same as the time of peak effect. Thus, the difference between peak times for effect and plasma concentrations provides the time required for distribution to biophase to be complete. Distribution is a first-order process governed by first-order rate constant k_{e0}. Thus, it

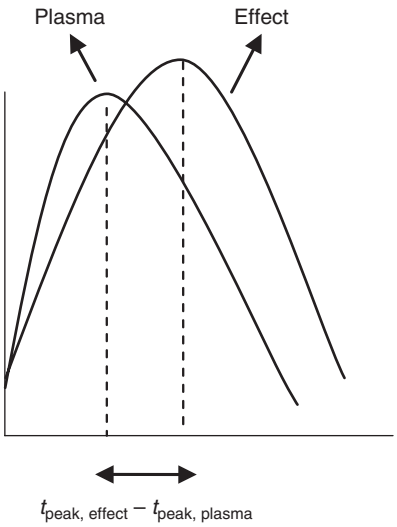

Figure 17.16 Determination of initial estimate of k_{e0}.

would take approximately four $t_{1/2,k_{e0}}$ for the distribution to complete. Hence, k_{e0} is calculated from Equations 17.22 and 17.23. An estimate of E_{max} can be obtained from the maximal response. EC_{50} estimate can obtained from concentration at $\frac{1}{2}E_{max}$ on down-curve of hysteresis arm:

$$t_{1/2,k_{e0}} = \frac{(t_{peak,effect} - t_{peak,plasma})}{4} \tag{17.22}$$

$$k_{e0} = \frac{0.693}{t_{1/2,k_{e0}}} \tag{17.23}$$

17.7.1.2.2 Indirect Response Models. "Indirect response" refers to a PD response that is produced when the drug acts on the production or dissipation of the endogenous factors that affect/control the response [53].

The basic equation for the scheme is provided below:

$$\frac{dR}{dt} = k_{in} - k_{out} \cdot R \tag{17.24}$$

where k_{in} is the zero-order production rate of response, R, and k_{out} is the first-order rate constant for the loss of response. Usually, R is measured as graded or continuous variable (Section 17.5). R begins at a baseline value and changes with time when a drug is administered and reaches back to its baseline value after the drug is out of the system.

When no drug is present, R has the baseline value R_0, which is obtained by putting $dR/dt = 0$. Thus, $R_0 = k_{in}/k_{out}$.

For the basic indirect response models, four possibilities have been described (Fig. 17.17) [54]. The drug either inhibits or stimulates production or loss of response.

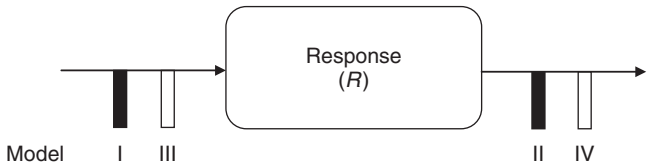

Figure 17.17 Schematic diagram for four basic indirect response models. Black solid bar indicates inhibitory function and white bar indicates stimulatory function.

The effect of the drug on the system can be asserted with the aid of a stimulatory or an inhibitory response. An inhibitory or a stimulatory response can be depicted as $I(t)$ and $S(t)$:

$$I(t) = 1 - \frac{I_{\max} \cdot C}{\mathrm{IC}_{50} + C} \tag{17.25}$$

$$S(t) = 1 + \frac{S_{\max} \cdot C}{\mathrm{SC}_{50} + C} \tag{17.26}$$

In these equations, C represents the plasma/blood concentrations of the drug. $\mathrm{IC}_{50}/\mathrm{SC}_{50}$ is the concentration of the drug at half the maximal inhibitory/stimulatory effect. $E_{\max}$ or $S_{\max}$ represents the maximum effect of the drug on the response.

In the inhibitory equation, $I(t)$ assumes that $0 < I_{\max} \geq 1$. If the drug concentration is high enough to produce maximum inhibition of either production or loss of response, $I_{\max}$ is assigned a value of 1. The equation, then, is written in the following form:

$$I(t) = 1 - \frac{C}{\mathrm{IC}_{50} + C} \tag{17.27}$$

MODEL I: INHIBITION OF PRODUCTION OF RESPONSE. The turnover equation for this model is as follows:

$$\frac{\mathrm{d}R}{\mathrm{d}t} = k_{\mathrm{in}} \cdot \left[1 - \frac{I_{\max} \cdot C}{\mathrm{IC}_{50} + C}\right] - k_{\mathrm{out}} \cdot R \tag{17.28}$$

The inhibition of production causes the response to decrease with time to a minimum value and then a gradual return to the predose baseline. Model I has been applied to a variety of drug responses in the literature. Some examples would be reduction of pain [55] and temperature [56] by anti-inflammatory drugs, effect of corticosteroids on cortisol [57], and effect of histamine H_2-receptor antagonists on the secretion of acid [58].

MODEL II: INHIBITION OF LOSS OF RESPONSE. The turnover equation for this model is as follows:

$$\frac{\mathrm{d}R}{\mathrm{d}t} = k_{\mathrm{in}} - k_{\mathrm{out}} \cdot \left[1 - \frac{I_{\max} \cdot C}{\mathrm{IC}_{50} + C}\right] \cdot R \tag{17.29}$$

For model II, the signature profile looks opposite of model I. Since the loss of response is inhibited as the response increases with time and returns back to baseline.

Model II has been reported in the literature for cholinesterase inhibition as well as inhibition of water reuptake by diuretics [59]. Inhibition of water reuptake leads to increased diuresis.

MODEL III: STIMULATION OF PRODUCTION OF RESPONSE. The turnover equation for model III is as follows:

$$\frac{dR}{dt} = k_{in} \cdot \left[1 + \frac{S_{max} \cdot C}{SC_{50} + C}\right] - k_{out} \cdot R \tag{17.30}$$

For model III, the drug stimulates the production of the response. Thus, the response increases from baseline with time and then returns back to the baseline. The signature profile is similar to that of model II. In the literature, model III has been applied to bronchodilatory effects of terbutaline [50], growth-hormone-releasing effect of ipamorelin [60], as well as induction of prolactin secretion by a dopamine receptor antagonist [61].

MODEL IV: STIMULATION OF LOSS OF RESPONSE. In model IV, the drug causes stimulation of the loss of response. Thus, the signature profile is similar to that of model I. The response decreases after drug administration and then trends back to the baseline levels as the drug is eliminated from the system.

The turnover equation of this system is as follows:

$$\frac{dR}{dt} = k_{in} - k_{out} \cdot \left[1 + \frac{S_{max} \cdot C}{SC_{50} + C}\right] \cdot R \tag{17.31}$$

Model IV has been applied to terbutaline's effect on lowering plasma potassium levels [59,62]. As the plasma concentrations for terbutaline increase, the plasma potassium concentrations decrease, the peak of decrease in potassium concentrations is delayed by approximately half an hour.

DIFFERENCE BETWEEN BIOPHASE/LINK MODEL AND INDIRECT RESPONSE MODELS. The movement of drug in and out of the hypothetical distribution compartment might apparently look similar to the processes k_{in} and k_{out}. For a data set that should be fitted with an indirect response model if fitted with a biophase/link model would perform equally well for a single dose. The fits, however, would become worse with simultaneous fitting of more than one dose levels to obtain a common set of parameters. One of the primary reasons lies in the basic expectations from the two models. For biophase/link models, the maximum effect is expected to occur at the same time, whereas for the indirect response models, the peak effect is further delayed with increasing doses [54]. Data simulated with indirect response models when fitted with a biophase model produces different values of parameters with data for different dose levels [63–65].

SIGNATURE PROFILES. Figure 17.18 shows signature profiles for the indirect response models. A pattern of decrease and return to baseline is observed with models I and IV. An opposite pattern, increase in response and return back to baseline, is observed with models II and III. With an increase in dose, all the parameters, maximum response, initial slope, and $T_{max,effect}$ also increase. The peak response is delayed with increase in dose [66,67].

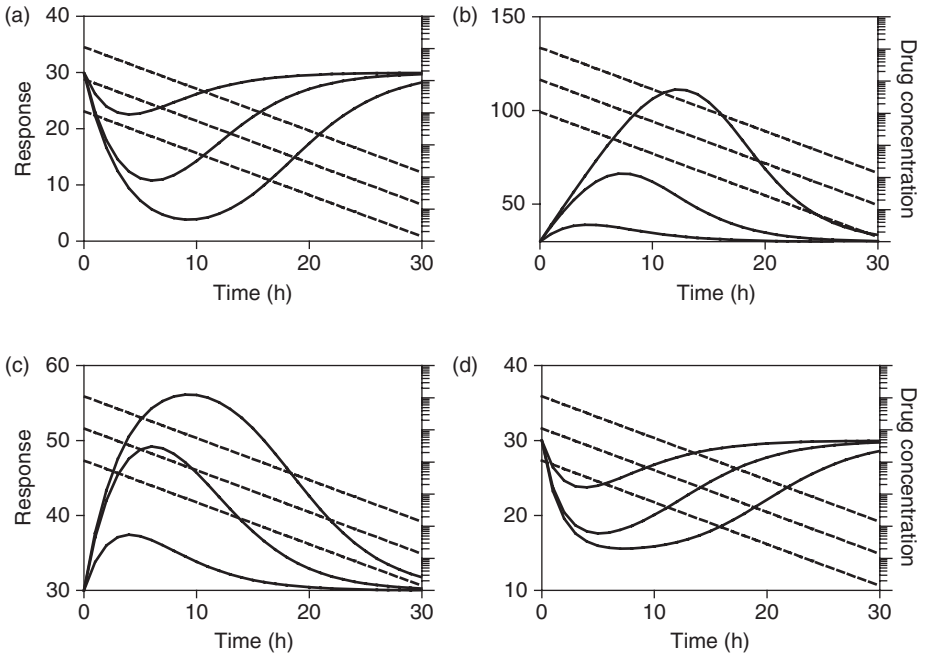

Figure 17.18 Signature profiles for four basic indirect response models. $V = 90$, $k_{el} = 0.3$, $I_{max} = 1$, $S_{max} = 1$, $SC_{50} = 100$, $IC_{50} = 100$, $k_{in} = 9$, $k_{out} = 0.3$, $R_0 = 30$. Doses: 10–1000 units. (a) Model I, (b) model II, (c) model III, and (d) model IV. *Source*: Parameters obtained from Ref. 67.

TABLE 17.3 Initial Parameter Estimates for Basic Indirect Response Models

Parameter	Model I	Model II	Model III	Model IV
I_{max}/S_{max}	$\frac{(R_0 - R_{max})}{R_0}$	$\frac{(R_{max} - R_0)}{R_0}$	$\frac{(R_{max} - R_0)}{R_0}$	$\frac{(R_0 - R_{max})}{R_0}$
k_{in}	$-\frac{S_I}{I_{max}}$	$\frac{S_I}{I_{max}}$	$\frac{S_I}{S_{max}}$	$-\frac{S_I}{S_{max}}$
k_{out}	$\frac{k_{in}}{R_0}$	$\frac{k_{in}}{R_0}$	$\frac{k_{in}}{R_0}$	$\frac{k_{in}}{R_0}$
IC_{50}/SC_{50}	See Ref. 58 for the initial estimates for IC_{50}/SC_{50}			

INITIAL PARAMETER ESTIMATES. The details of initial parameter estimates have been provided by Sharma and Jusko [66]. Table 17.3 contains the equations to calculate the initial estimates.

17.7.1.2.3 Cell Life Span Models. This type of model has mainly found its application in the effect of substances, which stimulate the growth of cells in the body like the hematopoietic cells (RBC, etc.). Cell life span is defined as the time a cell spends in a population. Cell life span models assume that the loss of response (population of cells)

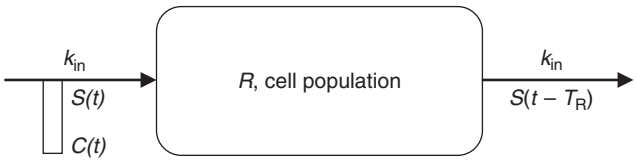

Figure 17.19 Basic one-pool cell model.

does not follow first-order processes but occurs due to natural senescence. A population of cells, R is controlled by two processes, a production rate and a loss rate [68]. Production can be due to physiological processes such as cell division, differentiation, and maturation, whereas cell loss may be due to senescence and random conversion to another type, such as hematopoietic cells. The following is the basic equation for the turnover of a cell population:

$$\frac{dR}{dt} = \text{production}(t) - \text{loss}(t) \tag{17.32}$$

Figure 17.19 shows a basic one-pool cell model. As mentioned previously, the loss process is assumed to be dependent on either natural senescence or conversion to another type of cells. Each cell lives for a specific period of time (T_R) and then dies or becomes another cell. The number of cells disappearing in a given time interval is equal to the number of cells generated. Or, the production rate is equal to that of the loss rate but delayed by T_R:

$$\text{Loss rate} = \text{production rate } (t - T_R)$$

The drug stimulates the production of response, which here is the cell population with a stimulatory function $S(t)$:

$$S(t) = \frac{S_{max} \cdot C^{\gamma}}{SC_{50}^{\gamma} + C^{\gamma}} \tag{17.33}$$

where C is the concentration of the drug in the cell compartment, S_{max} is the maximum extent to which the production of cells can be achieved, and SC_{50} corresponds to the concentration at which the drug exhibits 50% stimulation of cell population. A Hill coefficient, γ, may be required to adjust for the shape of the response or can be set equal to one.

In this system, the production rate is described by the following equation:

$$\text{Production}(t) = k_{in} \cdot S(t) \tag{17.34}$$

Since loss rate is delayed by the life span of the cell (T_R), the equation for loss rate would be as follows:

$$\text{Loss}(t) = k_{in} \cdot S(t - T_R) \tag{17.35}$$

Thus, the basic one-pool cell model can be described by Equation 17.36:

$$\frac{dR}{dt} = \frac{k_{in} \cdot S_{max} \cdot C(t)^{\gamma}}{SC_{50}^{\gamma} + C(t)^{\gamma}} - \frac{k_{in} \cdot S_{max} \cdot C(t - T_R)^{\gamma}}{SC_{50}^{\gamma} + C(t - T_R)^{\gamma}} \tag{17.36}$$

$k_{in} \cdot S_{max}$ may be written as S_m and represents the maximum rate of cell production by the drug.

BASELINE (R_o). In the one-pool cell model depicted above, the production rate is equal to the loss rate and only delayed by the life span of the cell. The cells are produced by a zero-order rate constant k_{in}, which indicates that the number of cells born does not depend on the pool, R. In this scenario, the baseline value would be the same and not depend on any system parameters.

Thus, the value for the baseline was derived by Krzyzanski *et al*. [68] by assuming the production of cells was shut down. The equation thus obtained for the baseline is then expressed as follows:

$$R_0 = k_{in} \cdot T_R \tag{17.37}$$

PRESENCE OF AN ENDOGENOUS ACTIVE SUBSTANCE. If an endogenous compound stimulates the cell population, the baseline equation does not remain the same. Assuming a concentration of the endogenous compound to be C_0, the baseline equation will now be basally stimulated as follows:

$$R_0 = k_{in} \cdot T_R \cdot \left(1 + \frac{S_{max} C_0^{\gamma}}{EC_{50}^{\gamma} + C_0^{\gamma}}\right) \tag{17.38}$$

SIGNATURE PROFILES. Figure 17.20a depicts the PK profiles of an agent which stimulates the production of cell population. PK was assumed to be one compartment with first order elimination with IV bolus dosing. Figure 17.20b depicts signature profiles for one-pool cell life span model for three dose levels. The rising part of the curves is entirely dependent on the production rate in an apparent zero-order manner. The profile reaches the peak exactly at the life span of the population [68]. After reaching its peak, the loss rate takes over and the response reaches the baseline. Figure 17.20c depicts the profiles at different values of T_R. As the values of T_R increase, the peak appears later as expected since the model predicts the peak to appear at T_R.

INITIAL ESTIMATES.

$$T_R = T_{max}$$

$$k_{in} = \frac{R_0}{T_R}$$

$$S_{max} = \frac{R_{max}}{R_0} - 1$$

$$S_I = k_{in} \cdot S_{max}$$

The estimate of S_{max} is reliable only at large doses since at smaller doses, true maximum effect is not achieved. S_I is the maximal initial slope.

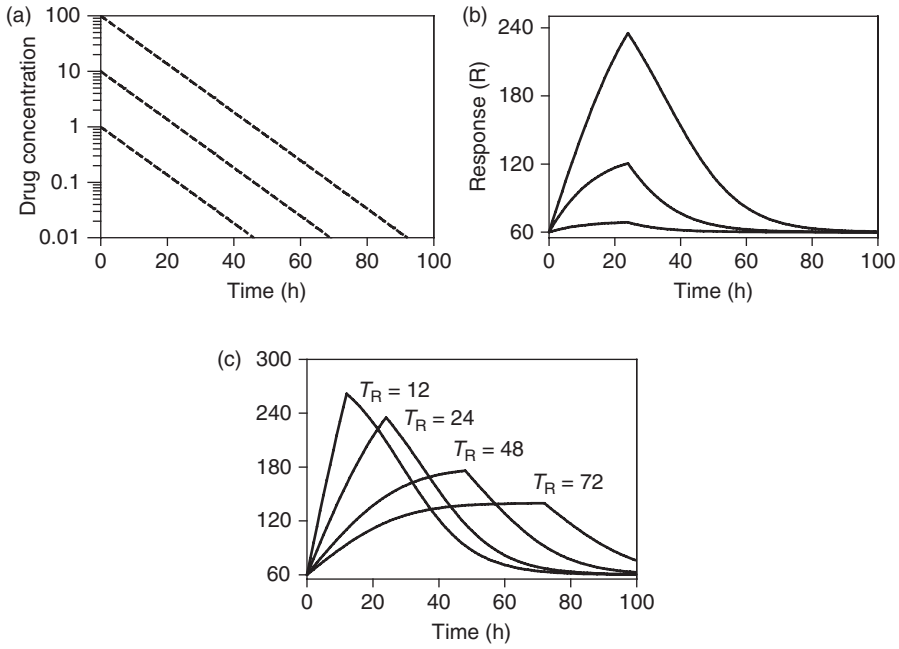

Figure 17.20 Signature profiles for one-pool cell life span model. $k_{el} = 0.1$; $V = 1$; dose = 1, 10, and 100; $T_R = 24$; $S_{max} = 4$; $SC_{50} = 10$; and $\gamma = 1$. *Source*: Parameters obtained from Ref. 69.

APPLICATION OF CELL LIFE SPAN MODELS. Cell life span models have been applied mainly to drugs that alter the production of hematopoietic cells [69–76]. Woo *et al*. [74] studied the effects of recombinant human erythropoietin (rHuEPO) on reticulocytes, RBC, hemoglobin, and mean corpuscular hemoglobin (MCH) in rats. The four-pool cell life span model appropriately described the change in the PD parameters and generated life span values for two precursor compartments as well as for reticulocytes. To date, cell life span concepts have been only applied in case of rHuEPO and in one case for thrombopoietin (TPO) and recombinant human granulocyte colony stimulating factor (rHuG-CSF) [68].

17.7.1.2.4 Time-Dependent Transduction Models. Time-dependent transduction models have been used to describe the underlying mechanism for a delayed PD response as signal transduction or some unknown mechanism. Signal transduction is the process by which a cell converts an extracellular signal into a response. A typical signal-transduction process is shown in Fig. 17.21. The signal "s" enters the cell and binds to the receptor R. This signal–receptor complex can cause an immediate direct effect. On the other hand, the signal–receptor complex can also enter the nucleus and bind to the gene response element to cause a gene-mediated delayed effect. If the intermediate steps are not measured, the data could be modeled empirically with a transduction model. Ligands for nuclear hormone receptors, described in Section 17.2, cause signal-transduction cascade and can produce long delays in response. GPCRs and ion channels, on the other hand, do not produce this kind of long delays once a ligand binds to them. Figure 17.22 depicts typical PK-PD expectation for a time-dependent transduction model [77].

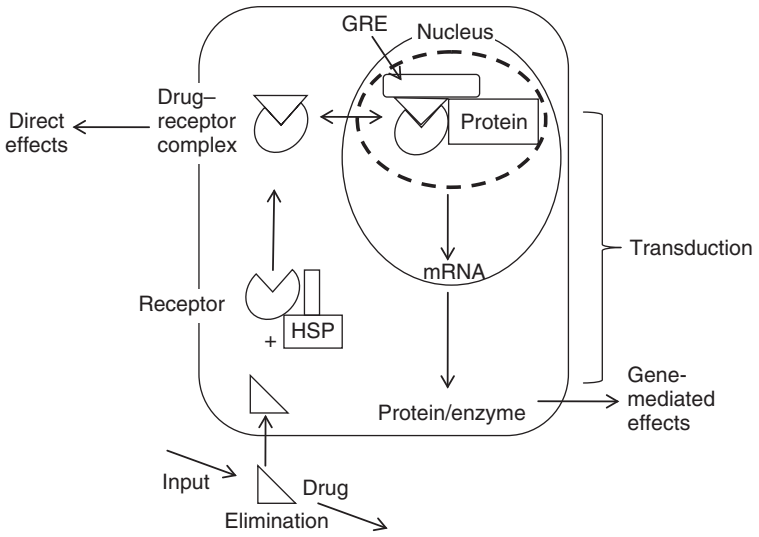

Figure 17.21 Schematic diagram for a signal-transduction process. *Source*: Adapted from Ref. 77.

The dotted line shows the PK profile and the solid line shows the PD profile. It is curious to note that the drug may be almost out of the system, but the PD marker is still at its baseline. In the case of biophase, indirect response (IDR), and cell life span models, the peak of the PD response appears later than the PK peak. However, in the case of transduction, one can see a significant delay, as depicted in (Fig. 17.22). Mathematically, the transit compartment technique is primarily used to model this delay between the PK and the PD response [78,79]. Figure 17.23 depicts a typical transit compartment model. $T_1, T_2, \ldots, T_N$ are the transit compartments. Mathematically, the transit compartment model contains a series of differential equations (Eqs. 17.39–17.42), which describe a cascade of events between target occupancy and the PD effect. τ is defined as the mean transit time of signal from one compartment to the other and is assumed to be the same for all the compartments. γ is the power coefficient, which amplifies or dampens the signal of the transducer and is analogous to the Hill coefficient.

INITIAL ESTIMATES. The number of transit compartments (N), mean transit time (τ), and the power coefficient (γ) should be determined by fitting the model to the data:

$$\frac{dR}{dt} = \frac{1}{\tau} \cdot \left(1 - \frac{I_{max} \cdot C}{IC_{50} + C} - R\right) \tag{17.39}$$

$$\frac{dT_1}{dt} = \frac{1}{\tau} \cdot (R - T_1) \tag{17.40}$$

$$\frac{dT_2}{dt} = \frac{1}{\tau} \cdot (T_1^{\gamma} - T_2) \tag{17.41}$$

$$\frac{dT_n}{dt} = \frac{1}{\tau} \cdot (T_{n-1} - T_n) \tag{17.42}$$

Figure 17.22 PK-PD expectation for a time-dependent transduction process. Dotted line, pharmacokinetics; solid line, pharmacodynamic expectation.

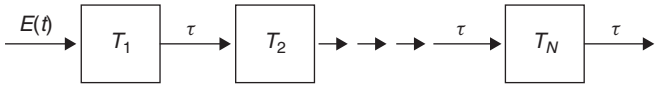

Figure 17.23 Transit compartment model for describing time-dependent transduction system.

SIGNATURE PROFILES. Figure 17.24 depicts the signature profiles for a single-step transduction process at different dose levels. The initial slope of these profiles is dose-independent. The time to peak effect is dose-dependent unlike biophase/link model. For medium to high dose levels, decline in response is parallel and inflection point represents the EC_{50}. The profiles mimic IDR model III (stimulation of k_{in}) for single-step processes but would not in case where multiple transduction processes exist. Figure 17.25a depicts the effect of increase in τ on the signature profiles for a transduction system. As τ increases, the profiles shift to later times and the maximum effect is diminished. Similarly, Fig. 17.25b depicts the effect of increase in the number of transduction compartments. The effect is similar to that of increase in τ. With an increase in the number of compartments, the profiles shift to later times and the maximum effect diminishes.

APPLICATIONS. Application of transduction models have been found in the literature in multiple therapeutic areas. These models have been applied to the cardiovascular area by Perlstein *et al*. [80]. A signal-transduction model with three delay compartments and a shape factor on the second compartment was used to capture the delay of the PD

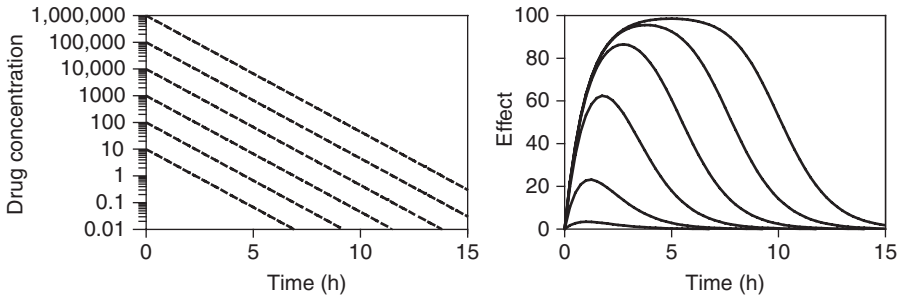

Figure 17.24 Signature profiles for single-step transduction process. $V = 0.1$; $k_{el} = 1$; $E_{max} = 100$; $EC_{50} = 100$; $\tau = 1$.

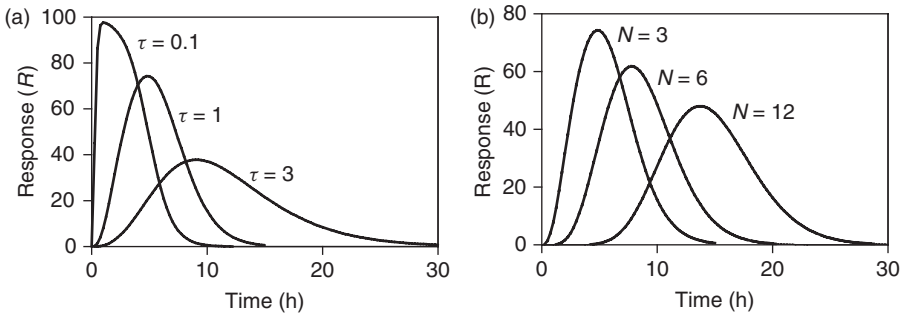

Figure 17.25 The effect of τ and N on the signature profiles for a transduction system. (a) Effect of increase in the values of τ and (b) effect of increase in the number of delay compartments (N).

response. Delays in tumor growth have also been described extensively in the oncology area [81–85]. Lobo and Balthasar [81] modeled the delay in tumor growth using the killing rate constant with transit compartments. Simeoni *et al*. modeled the delay by dividing the tumor compartment into four transit compartments and called them *injured tumor cells*. The sum of all the injured cell compartments and the tumor compartment will produce the final response that is invariably a decrease in tumor weight [82].

17.7.2 Irreversible Effects

Effects such as cell killing and enzyme inactivation are known as *irreversible effects*. The response returns to the baseline not due to turnover of the response but due to growth of cells or synthesis of new enzymes. These agents generally covalently bind to the target, which promotes the destruction of cells/enzymes.

17.7.2.1 Cell Kill Models. This type of model was first applied by Jusko [86] in 1971. Figure 17.26 depicts the basic structure of the model.

R is the PD response, which is the number of cells in a population. The growth rate of the cells (describe by kilograms) is a first-order process and depends on the number of cells present in the population. The cells have their natural death governed by the first-order rate constant k. C represents the concentrations of the chemotherapeutic

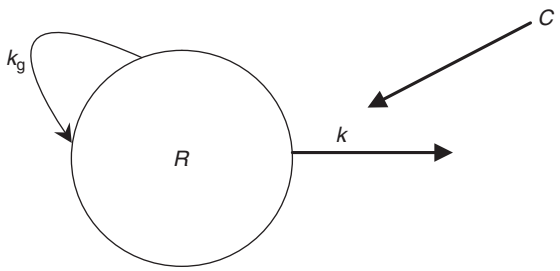

Figure 17.26 Basic structure of a cell killing model.

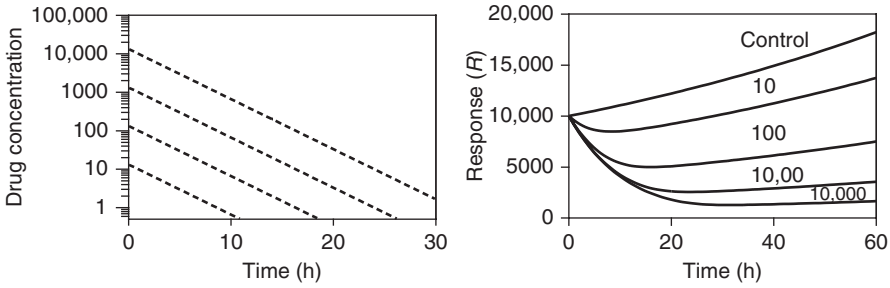

Figure 17.27 Signature profiles for a cell killing model with nonlinear killing function. $V = 0.75$, $k_{el} = 0.3$, $k_g = 0.01$, $K_{max} = 0.1$, $KC_{50} = 10$. Dose = 0, 10, 100, 1000, and 10,000 units.

agent that stimulates cell death. The equation for this type of system is provided below:

$$\frac{dR}{dt} = k_g \cdot R - k \cdot C \cdot R \tag{17.43}$$

Integration of the above equation gives

$$R = R_0 \cdot e^{k_g t} \cdot e^{-k \cdot AUC_0^t} \tag{17.44}$$

Looking at the above equation, one might mistakenly think that killing of the cells is independent of time, but the time component is hidden in the AUC term.

Instead of a linear cell kill constant, a nonlinear cell kill constant can be used as well. The rate constant for killing, k, will be modified to the following equation:

$$k = \frac{K_{max} \cdot C}{KC_{50} + C} \tag{17.45}$$

Signature profiles for the cell killing model with a nonlinear kill rate function are depicted in (Fig. 17.27). Monoexponential decline of PK was assumed. The PD profiles show decline in response and the response returns beyond the baseline as one would expect since the response in proliferating cells grows when there is no drug in the system. The control curve, on the other hand, only grows since there in no drug in the system to kill the cells.

17.7.2.1.1 Initial Estimates. Figure 17.28 shows the method of determination of initial estimates from the model.

In Fig. 17.28, plotted on the Y-axis is the log of survival fraction (R/R_0) and plotted on the X-axis is time. The initial estimates for k_g and k are obtained from the following equations, where t_D is the doubling time of the cells and can be obtained from observed data:

$$k = -\frac{\ln S_F}{AUC_0^t} \tag{17.46}$$

$$k_g = \frac{0.693}{t_D} \tag{17.47}$$

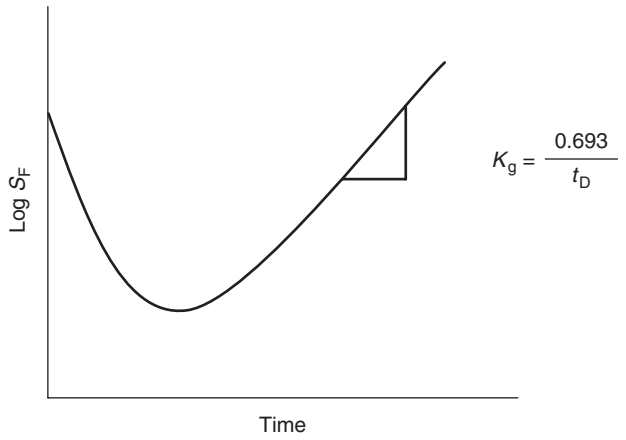

Figure 17.28 Method for obtaining initial estimates for a basic cell kill model.

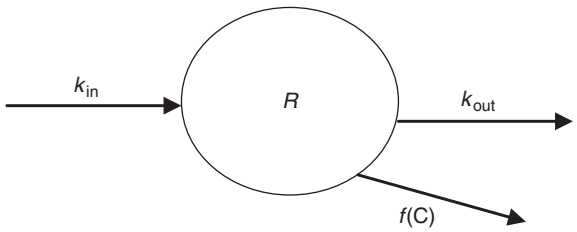

Figure 17.29 An irreversible enzyme inactivation model.

17.7.2.1.2 Applications. These models have been applied [87] to effect of piperacillin in studies of neutropenic mice infected with *Pseudomonas aeruginosa*. For all the doses, the survival fraction goes down, and as the drug is eliminated, the bacteria continues to grow again.

17.7.2.2 Model for Enzyme Inactivation. The structure of a typical enzyme inactivation model is depicted in Fig. 17.29.

R represents the enzyme concentrations. The enzyme is produced by a zero-order rate constant k_{in} and a first-order rate constant k_{out}. $f(C)$ represents the irreversible effect of the drug on the turnover of the enzyme. In absence of drug C, the model is similar to a turnover model, where $R_0 = k_{in}/k_{out}$. Equation 17.48 shows the turnover of the enzyme in presence of the drug. The effect of the drug can either be linear or represented by an E_{max} function. Equations 17.49 and 17.50 describe the two types of drug effect:

$$\frac{dR}{dt} = k_{in} - k_{out} \cdot R - f(C) \cdot R \tag{17.48}$$

$$f(C) = k \cdot C \tag{17.49}$$

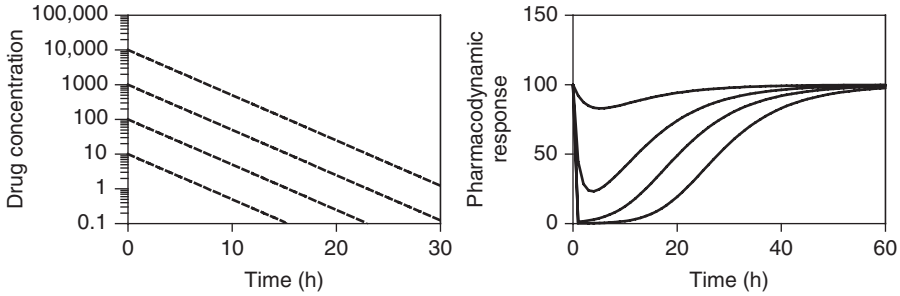

Figure 17.30 Signature profiles for an irreversible enzyme inactivation model. $k_{el} = 0.3$, $V = 1$, $k_{in} = 10$, $k_{out} = 0.1$, $k = 0.01$. Dose = 10, 100, and 1000 units.

$$f(C) = \frac{K_{max} \cdot C}{KC_{50} + C} \tag{17.50}$$

17.7.2.2.1 Signature Profiles. Figure 17.30 depicts the signature profiles for enzyme inactivation model at a range of doses. The response declines from baseline to a minimum and returns back to the baseline with time. There is a dose-dependent shift in the maximal effect; however, the peak effect occurs earlier unlike indirect response models, where peak effect occurs later at higher doses [88].

17.7.2.2.2 Applications. The basic turnover-irreversible model has been applied to inhibition of gastric acid secretion of pantoprazole [89]. This model was further used to simulate reduction in acid secretion at 40-mg dose to validate the model. The model was further validated by integration of clinical data, which showed reduction in time to maximal effects with an increase in concentrations or dose as well as higher infusion rates. This kind of model has also been applied to antiplatelet effects of aspirin [90].

17.7.3 Other Models

17.7.3.1 Disease Progression Models. Clinical pharmacology is a combination of how a disease progresses and the effect of drug on the progression of disease. It was first indicated by Holford and Sheiner in 1981 that the baseline in patients, which we use in an E_{max} model (E_0), is not a constant number. The change in E_0 over time should be taken into consideration while analyzing the clinical data [91]. The progression of disease refers to time course or trajectory of a biomarker or a PD or clinical end point, which is a measure of the clinical status of the patient. This trajectory of the disease progression can be linear, nonlinear, or cyclical. Thus, a model for progression of a disease should incorporate these factors with mathematical function to describe the time course of disease progression [92]. Also, there may be situations where the disease conditions change the underlying PK and PD. These changes should also be incorporated during analysis of clinical data and clinical trial simulations.

17.7.3.1.1 Effects of Drugs in Disease Progression. The effect of a drug on the disease progression may be of three types [93]. Figure 17.31 depicts the three types of drug effects on disease progression.

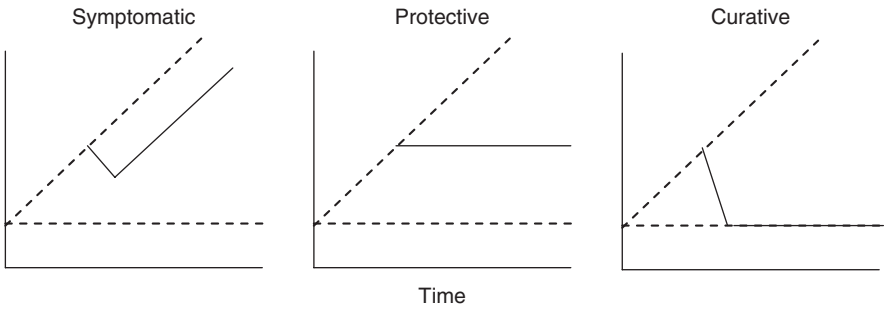

Figure 17.31 Types of effects of different drugs on disease progression.

SYMPTOMATIC. The effect of a drug is named symptomatic if it has a beneficial effect on the disease but does not change the underlying process of the disease or the trajectory of the disease. The drug delays the progression of the disease, and as the drug exits the system, the disease follows its normal path. This type of drug effect has been seen with tacrine in the treatment of Alzheimer's disease [94]. The drug delays the deterioration of the patient by six months, and as soon as the therapy is stopped, the deterioration follows its natural path.

DISEASE MODIFYING OR PROTECTIVE. A drug is said to be protective or disease modifying if it interferes with the natural history or trajectory of the disease and causes a permanent change. Thus, the effect remains even after the drug has been eliminated or therapy has been stopped. Protective effects may be of two types, one which alters the time course of progression of the disease and the other which changes the maximal status of the disease.

CURATIVE. The effect of a drug is said to be curative if the therapy completely arrests the progression of the disease. Again, removal of drug from the system or stopping of therapy keeps the patient in the state before the disease started [92]. Chemotherapeutic agents such as antibacterial agents and some anticancer agents exhibit curative effects.

17.7.3.1.2 Models of Disease Progression.

LINEAR MODELS. The linear model of disease progression is the simplest model used to describe the time course of progression of several diseases. The model assumes that the patient has a baseline disease condition S_0 and a slope α, which is responsible for the change in the disease condition with time. Equation 17.51 shows the disease model without the effect of the drug:

$$S(t) = S_0 + \alpha \cdot t \tag{17.51}$$

A disease progression model is built in two steps. First, the model for the disease is built and then the effect of the drug is added to it. Equation 17.52 shows the effect of the drug $[f(C)]$:

$$S(t) = S_0 + \alpha \cdot t + f(C) \tag{17.52}$$

Equation 17.52 shows a symptomatic drug effect on the disease. The drug does not act on α. Once the therapy is stopped or the drug goes out of the system, the same slope α resumes. Equation 17.53, on the other hand, shows the protective effect of the drug. In this case, the drug acts on the slope α, and at the end of therapy, the value of α changes to a different value, α′:

$$S(t) = S_0 + (\alpha + f(C)) \cdot t \tag{17.53}$$

ASYMPTOTIC MODELS. The linear models have their own disadvantages. They are useful for time frames that are mainly linear. Also, the biological systems, more often than not, change nonlinearly with time. Thus, asymptotic models are often used to describe a variety of diseases. There are different kinds of asymptotic models used in the literature to describe different disease processes. These models are named so since they are associated with some kind of plateau of the disease biomarker. Table 17.4 depicts different types of disease models and the effect of drugs on the disease.

Apart from the examples shown in Table 17.4, other asymptotic models can be used such as inverse Bateman function [92] and cyclical modification of inverse Bateman function [92].

GROWTH MODELS. Apart from all the linear and asymptotic models, different types of growth models have also been used to describe disease progression. A Gompertz-type growth function has been used to describe the time course of Parkinson's disease [92], as depicted in the following equation:

$$\frac{dR}{dt} = \beta \cdot R \cdot (\beta_{max} - R) - (k_{death} \cdot R) \tag{17.54}$$

In addition to these models, transit compartment models have also been used to describe a time course of disease [92].

TABLE 17.4 Asymptotic Models of Disease Progression and Effect of Drug on Disease

Model	Equation	Symptomatic Drug Effect	Disease Modifying or Protective Drug Effect	References
Exponential	$S(t) = S_0 \cdot e^{-k_{PROG} \cdot t}$	$S(t) = S_0 \cdot e^{-k_{PROG} \cdot t} - f(C)$	$S(t) = S_0 \cdot e^{-[k_{PROG} + f(C)]t}$	87
E_{max} function	$S(t) = S_0 + \frac{S_{max} \cdot t}{SC_{50} + t}$	$S(t) = S_0 + \frac{S_{max} \cdot t}{SC_{50} + t} \pm f(C)$	$S(t) = S_0 + \frac{S_{max} \cdot [1 + f(C)] \cdot t}{SC_{50} \cdot [1 + f(C)] + t}$	88,89
Nonzero asymptotic function	$S(t) = S_0 \cdot e^{-k_{PROG} \cdot t} + S_{ss} \cdot (1 - e^{-k_{PROG} \cdot t})$	$S(t) = S_0 \cdot e^{-k_{PROG} \cdot t} + S_{ss} \cdot (1 - e^{-k_{PROG} t}) \pm f(C)$	$S(t) = S_0 \cdot e^{-k_{PROG} \cdot [1 + f(C)] \cdot t} + S_{ss} \cdot (1 - e^{-k_{PROG} \cdot [1 + f(C)] \cdot t})$	84

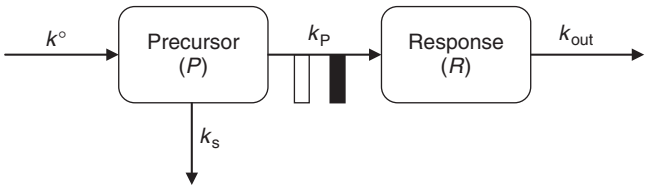

Figure 17.32 Schematic diagram of a precursor-dependent indirect response model.

17.7.3.2 Models of Tolerance and Rebound. As defined in Section 17.2, tolerance is referred to as a *phenomenon where the response to the drug exposure is diminished due to repeated administration of the drug*. This phenomenon might be observed in the clinic as well as in preclinical species and has been described by the following PD models.

17.7.3.2.1 Precursor-Dependent Indirect Response Model. This model describes the phenomenon of tolerance and rebound in case of indirect PD responses. The model in general shows how a drug can affect a precursor pool by stimulation or inhibition of the elimination of the precursor. The structure of the model is depicted in (Fig. 17.32). Precursor P is synthesized by a zero-order rate k_0 and lost by the first-order rate k_S. Precursor is converted to response R by a first-order rate k_P. The response, R, is dissipated by a first-order rate k_{out} [95]. The drug either stimulates or inhibits the conversion of the precursor to the response by inhibitory $I(t)$ or stimulatory $S(t)$ functions as follows. The rate of change of response and the precursor can be described by the following set of differential equations:

$$\frac{dP}{dt} = k^{\circ} - k_P(1 \pm H(t)) \cdot P - k_S \cdot P \tag{17.55}$$

$$\frac{dR}{dt} = k_P(1 \pm H(t)) \cdot P - k_{out} \cdot R \tag{17.56}$$

$H(t)$ represents either stimulatory or inhibitory Hill functions, as described by the following equations:

$$S(t) = 1 + \frac{S_{max} \cdot C}{SC_{50} + C} \tag{17.57}$$

$$I(t) = 1 - \frac{I_{max} \cdot C}{IC_{50} + C} \tag{17.58}$$

The signature profiles for the stimulation model after four doses starting from 10 units to 10,000 units are shown in Fig. 17.33. In precursor-dependent IDRs, rebound is mainly due to depletion (stimulation model) or accumulation (inhibition model) in the amount of precursor with time, flowing into the drug compartment. The maximal effect increases with increase in dose. The effect reaches the baseline and further goes down producing rebound. The peak of the rebound shifts toward later time points with dose. Figure 17.34 depicts the effect of multiple dosing on the signature profiles of a

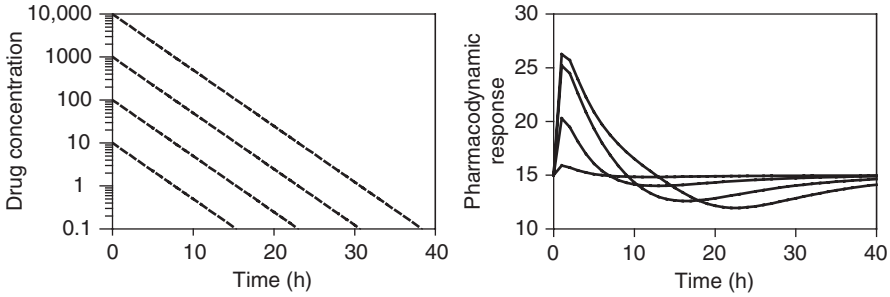

Figure 17.33 Signature profiles from a precursor-dependent indirect response model. $k_{el} = 0.3$, $V = 1$, $R_0 = 15$, $P_0 = 300$, $k_p = 0.1$, $k_s = 0$, $k_{out} = 2$, $E_{max} = 1$, $EC_{50} = 100$.

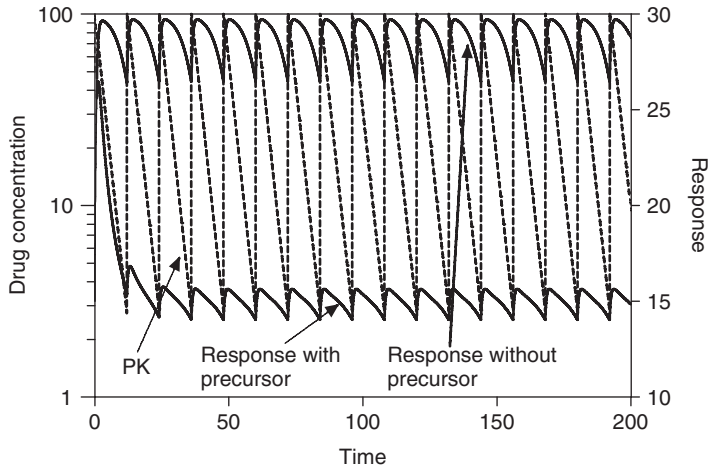

Figure 17.34 Development of tolerance during multiple dosing for a precursor-dependent IDR. Dose of 100 units given at an interval of 12 h. Dotted line, multiple dose pharmacokinetics; solid lines, multiple dose pharmacodynamics for models with and without precursor.

precursor-dependent indirect response model. Plotted in the same graph is the mono-exponential PK profiles and two PD profiles, one with the precursor compartment and the other without precursor compartment. The profile without the precursor compartment increases with multiple dose and reaches steady state as the PK reaches steady state with a slight delay in the peak times. When a precursor compartment is added, the PD response decreases with the first three doses and then achieves a steady state with response values much less than that achieved by the model without a precursor compartment. Thus, the model with a precursor compartment exhibits tolerance with multiple doses.

17.7.3.2.2 Counterregulatory Model. This type of model relies on the opposing effect acting on the response. The formation of the modulator is dependent on the response and a first-order rate constant, k_1, and dissipates with the rate constant k_2.

The turnover of the modulator is provided by the following equation:

$$\frac{dM}{dt} = k_1 \cdot R - k_2 \cdot M \tag{17.59}$$

The modulator compartment is then introduced into the mechanistic PD model as an opposing effect. The following equation shows such a modulator effect on an indirect response model:

$$\frac{dR}{dt} = k_{in} - k_{out} \cdot \left[1 - \frac{I_{max} \cdot C}{IC_{50} + C}\right] \cdot R \cdot (1 + M) \tag{17.60}$$

Counterregulatory models in their various forms have been used a multiple times in the literature [96,97]. Bauer and Fung developed a counterregulatory model to account for the effect and generation of tolerance by nitroglycerine in a rat model [97]. Counterregulatory mechanisms have been introduced in the indirect response model of diuresis to account for tolerance development by furosemide [97].

17.8 TOOLS AND SOFTWARES COMMONLY USED IN PK-PD MODELING

PK-PD modeling requires a computer to undergo iterative procedure to generate PK and PD parameters. Various softwares have been used from the inception of this kind of data analysis. Various softwares used are WinNonlin, ADAPT II and V, Matlab (extensively used in chemical engineering as well), SAAM II, Phoenix, and SAS for individual analysis. For population modeling, more popular softwares are NONMEM, S-ADAPT, R, S-PLUS, SAS, WinNonmix, ADAPT V, and Phoenix. For simulations, Berkeley Madonna is extensively used. Simulations for this chapter were performed with WinNonlin [98], ADAPT V [99], and Berkeley Madonna [100]. GraphPad Prism [101] was used for plotting the simulated data.

17.9 CONCLUSIONS

In order to perform and apply PK-PD modeling successfully, one requires a sound understanding of various disciplines such as biology, pharmacology, and mathematical and statistical sciences. Knowledge of biology and pharmacology helps in understanding a disease and therefore choosing the right biomarker for the development of a disease model. Modeling has diverse applications in both drug discovery and development, starting from understanding of efficacy animal models through dose selection for FIH studies, and throughout drug development.

17.10 FUTURE PERSPECTIVES: SYSTEMS MODELING

A recent interest in the area of PK-PD modeling is the development and application of systems modeling in drug discovery and development. Systems modeling refer to modeling a system such as heart or lung using same mathematical principles as used

in classical PK-PD modeling. Modeling has been thriving on applied mathematics to understand the quantitative relationship between kinetics of drug in the body and its effect [102]. Systems model mainly refer to the development of physiologically based disease progression models to which a drug effect can be incorporated. Modeling efforts in physiology have resulted in organ models such as the human lung model [103] and the lumped heart model [104]. Building similar systems with progression of disease is the latest challenge in PK-PD modeling. Once such a model has been built, drug effect can easily be incorporated. Some initial efforts have been made in this area recently by Landersdorfer and Jusko [105] and Danhof and colleagues [106]; however, the area is still in its evolution stage. A recent white paper from NIH states that, "quantitative systems pharmacology will create understanding of disease mechanisms and therapeutic effects that span biochemistry and structural studies, cell and animal-based experiments and clinical studies in human patients" [107].

ACKNOWLEDGMENTS

The authors would like to thank Dr. William J. Jusko, PhD, since materials from his publications were extensively referred in the preparation of this chapter. The authors thank their colleagues within Bristol-Myers Squibb, US, Punit Marathe, PhD, Michael Sinz, PhD, and Joseph Raybon, PhD, and also thank Jasminder Sahi, PhD, for their valuable suggestions and comments.

REFERENCES

1. Buxton ILO. Pharmacokinetics and pharmacodynamics. In: Brunton LL, Lazo JS, Parker KL, editors. Goodman and Gilman's: the pharmacological basis of therapeutics. 11th ed. New York: McGraw-Hill; 2006. pp. 1–39.
2. Hill AV. The possible effects of the aggregation of the molecules of hemoglobin on its dissociation curves. J Physiol 1910;40:iv–vii.
3. Holford NHG, Sheiner LB. Kinetics of pharmacological response. Pharmacol Ther 1982;16:141–166.
4. Clark AJ. The reaction between acetylcholine and muscle cells. J Physiol 1926;61: 530–546.
5. Levy G. Relationship between rate of elimination of tubocurarine and rate of decline of its pharmacological activity. Brit J Anaesthesiol 1964;36:694–695.
6. Segre G. Kinetics of interaction between drugs and biological systems. Farmaco Edizio Sci 1968;23:907–918.
7. Neubig RR, Spedding M, Kenakin T, *et al*. International union of pharmacology committee on receptor nomenclature and drug classification. XXXVIII. Update on terms and symbols in quantitative pharmacology. Pharmacol Rev 2003;55:597–606.
8. Zambrowicz BP, Sands AT. Knockouts model the 100 best-selling drugs-will they model the next 100? Nat Rev Drug Discov 2003;2(1):38–51.
9. Imming P, Sinning C, Meyer A. Drugs, their targets and the nature and number of drug targets. Nat Rev 2006;5:821–834.
10. Overington JP, Al-Lazikani B, Hopkins AL. How many drug targets are there? Nat Rev 2006;5:993–996.
11. Ashcroft FM. From molecule to malady. Nature 2006;440:440–447.
12. Camerino DC, Tricarico D, Desaphy JF. Ion channel pharmacology. Neurotherapeutics 2007;4(2):184–198.

13. Yokoshiki H, Sunagawa M, Seki T, *et al*. ATP-sensitive K^+ channels in pancreatic, cardiac, and vascular smooth muscle cells. Am J Physiol Cell Physiol 1998;274:C25–C37.
14. NuezVeulens VADL, Rodrrguez R. G protein-coupled receptors as targets for drug design. Biotecnol Aplicada 2009;26:24–33.
15. Gether U. Uncovering molecular mechanisms involved in activation of G protein-coupled receptors. Endocrine Rev 2000;21:90–113.
16. Rasmussen SG, DeVree BT, Zou Y, *et al*. Crystal structure of the β2 adrenergic receptor-Gs protein complex. Nature 2011;477(7366):549–555.
17. Landry Y, Gies JP. Drugs and their molecular targets: an updated overview. Fundam Clin Pharmacol 2008;22:1–18.
18. Hunter T. Tyrosine phosphorylation: thirty years and counting. Curr Opin Cell Biol 2009;21:140–146.
19. Schlessinger J. Cell signaling by receptor tyrosine kinases. Cell 2000;103:211–225.
20. Bagamasbad P, Denver RJ. Mechanisms and significance of nuclear receptor auto- and cross-regulation. Gen Comp Endocrinol 2011;170:3–17.
21. Germain P, Staels B, Dacquet C, *et al*. Overview of nomenclature of nuclear receptors. Pharmacol Rev 2006;58:685–704.
22. Furchgott RF. The use of b-haloalkylamines in the differentiation of receptors and in the determination of dissociation constants of receptor-agonist complexes. Adv Drug Res 1966;3:21–55.
23. Bakker RA, Wieland K, Timmerman H, *et al*. Constitutive activity of the histamine H(1) receptor reveals inverse agonism of histamine H(1) receptor antagonists. Eur J Pharmacol 2000;387(1):R5–R7.
24. Surin A, Pshenichkin S, Grajkowska E, *et al*. Cyclothiazide selectively inhibits mGluR1 receptors interacting with a common allosteric site for non-competitive antagonists. Neuropharmacology 2007;52(3):744–754.
25. Gool AJ, Henyr B, Sprengers ED. From biomarker strategies to biomarker activities and back. Drug Discov Today 2010;15(3/4):121–126.
26. Atkinson AJ, Colburn WA, DeGruttola VG, *et al*. Biomarkers and surrogate endpoints: Preferred definitions and conceptual framework. Clin Pharmacol Ther 2001;69:89–95.
27. Wagner JA. Strategic approach to fit-for-purpose biomarkers in drug development. Annu Rev Pharmacol Toxicol 2008;48:631–651.
28. Ross JS, Fletcher JA, Linette GP, *et al*. The Her-2/neu gene and protein in breast cancer 2003: biomarker and target of therapy. Oncologist 2003;8(4):307–325.
29. Yao Z, Hoffman EP, Ghimbovschi S, *et al*. Mathematical modeling of corticosteroid pharmacogenomics in rat muscle following acute and chronic methylprednisolone dosing. Mol Pharm 2008;5(2):328–339.
30. Hargreaves RJ. The role of molecular imaging in drug discovery and development. Clin Pharmacol Ther 2008;83(2):349–353.
31. Lathia CD, Amakye D, Dai W, *et al*. The value, qualification, and regulatory use of surrogate end points in drug development. Clin Pharmacol Ther 2009;86:32–43.
32. US Food and Drug Administration. Innovation or stagnation: challenge and opportunity on the critical path to new medical products. Available at http://www.fda.gov/ScienceResearch/SpecialTopics/CriticalPathInitiative/CriticalPathOpportunitiesReports/ucm077262.htm (accessed on 10 April 2012).
33. Preparing the ground for the future European medicines agency. The European Medicines Agency Road Map to 2010. Available at http://www.emea.europa.eu/docs/en_GB/document_library/Report/2009/10/WC500004903.pdf.
34. Morgan P, Van Der Graaf PH, Arrowsmith J, *et al*. Can the flow of medicines be improved? Fundamental pharmacokinetic and pharmacological principles toward improving Phase II survival. Drug Discovery Today 2012;17:419–424.

35. Krishna R, Herman G, Wagner JA. Accelerating drug development using biomarkers: a case study with sitagliptin, a novel DPP4 inhibitor for type 2 diabetes. AAPS J 2008;10(2):401–409.
36. Maurer TS, Ghosh A, Haddish-Berhane N, *et al*. Pharmacodynamic model of sodium-glucose transporter 2 (SGLT2) inhibition: implications for quantitative translational pharmacology. AAPS J 2011. Epub ahead of print. DOI: 10.1208/s12248-011-9297-2.
37. Laere KV, Koole M, Bohorquez SMS, *et al*. Whole-body biodistribution and radiation dosimetry of the human cannabinoid type-I receptor ligand ^{18}F-MK-9470 in healthy subjects. J Nuclear Med 2008;49(3):439–445.
38. Liu Y, Tan N, Zhou YL, *et al*. High-sensitivity C-reactive protein predicts contrast-induced nephropathy after primary percutaneous coronary intervention. J Nephrol 2011. Epub ahead of print. DOI: 10.5301/jn.5000007.
39. Rosenkranz B. Biomarkers and surrogate endpoints in clinical drug development. Appl Clin Trials 2003;40:30–34.
40. Wensing G, Ochmann K, Boettchar M, *et al*. Pharmacodynamic effects of an angiotensin II receptor-antagonist in phase I-comparison between healthy subjects and patients with hypertension. Biomark Insights 2007;2:81–93.
41. Xia L, Lu J, Xiao W. Blockage of TNF-α by infliximab reduces CCL2 and CCR2 levels in patients with rheumatoid arthritis. J Invest Med 2011;59(6):961–963.
42. Henley DB, May PC, Dean RA, *et al*. Development of semagacestat (LY450139), a functional gamma-secretase inhibitor, for the treatment of Alzheimer's disease. Expert Opin Pharmacother 2009;10(10):1657–1664.
43. Kappos L, Radue EW, O'Connor P, *et al*. FREEDOMS Study Group. A placebo-controlled trial of oral fingolimod in relapsing multiple sclerosis. N Engl J Med 2010;362(5):387–401.
44. US Food and Drug Administration. Challenge and opportunity on the critical path to new medical products. FDA; 2004. Available at http://www.fda.gov/ScienceResearch/SpecialTopics/CriticalPathInitiative/CriticalPathOpportunitiesReports/ucm077262.htm.
45. Gabrielson J, Weiner D. Pharmacokinetic/pharmacodynamic data analysis: concepts and applications. 4th ed. Sweden: Swedish Pharmaceutical Press; 2006.
46. Ariens EJ. Affinity and intrinsic activity in the theory of competitive inhibition. Arch Int Pharmacodyn Ther 1954;99:32.
47. Furchgott RF. The pharmacology of vascular smooth muscle. Pharmacol Rev 1995;7:183–265.
48. Sheiner LB, Stanski DR, Vozeh S, *et al*. Simultaneous modeling of pharmacokinetics and pharmacodynamics: application to d-tubocurarine. Clin Pharmacol Ther 1979;25:358–371.
49. Hermann DJ, Egan TD, Muir KT. Influence of arteriovenous sampling on remifentanil pharmacokinetics and pharmacodynamics. Clin Pharmacol Ther 1999;65(5):511–518.
50. Galeazzi RL, Benet LZ, Sheiner LB. Relationship between the pharmacokinetics and pharmacodynamics of procainamide. Clin Pharmacol Ther 1976;20(3):278–289.
51. Sheiner LB, Stanski DR, Vozeh S, *et al*. Simultaneous modeling of pharmacokinetics and pharmacodynamics: application to d-tubocurarine. Clin Pharmacol Ther. 1979;25(3):358–371.
52. Tuk B, Herben VM, Mandema JW, *et al*. Relevance of arteriovenous concentration differences in pharmacokinetic-pharmacodynamic modeling of midazolam. J Pharmacol Exp Ther 1998;284(1):202–207.
53. Garg V, Khunvichai A. Mechanistic pharmacokinetic/pharmacodynamic models I. In: Williams PJ, Ette EI, editors. Pharmacometrics. New York: John Wiley and Sons, Inc.; 2007. pp. 583–605.
54. Dayneka NL, Garg V, Jusko WJ. Comparison of four basic models of indirect pharmacodynamic responses. J Pharmacokinet Biopharm 1993;21(4):457–478.

55. Garg V, Jusko WJ. Pharmacodynamic modeling of non-steroidal anti-inflammatory drugs: antipyretic effect of ibuprofen. Clin Pharmacol Ther 1994;56:406–419.
56. Garg V, Ermer JC, Korth-Bradley J, *et al*. Comparison of effect compartment and indirect response models for the analgesic effect of bromfenac in humans. Pharm Res 1996;13:S446.
57. Lew KH, Jusko WJ. Pharmacodynamic modeling of cortisol suppression from fluocortolone. Eur J Clin Pharmacol 1993;45:581–583.
58. Mathôt RA, Geus WP. Pharmacodynamic modeling of the acid inhibitory effect of ranitidine in patients in an intensive care unit during prolonged dosing: characterization of tolerance. Clin Pharmacol Ther 1999;60:140–151.
59. Jusko WJ, Ko HC. Physiological indirect response models characterize diverse types of pharmacodynamic effects. Clin Pharmacol Ther 1994;56:406–419.
60. Gobburu JVS, Agerssø H, Jusko WJ, *et al*. Pharmacokinetic-pharmacodynamic modeling of ipamorelin, a growth hormone releasing peptide, in human volunteers. Pharm Res 1999;16:1412–1419.
61. Movin-Osswald G, Hammarlund-Udenaes M. Prolactin release after remoxipride by an integrated pharmacokinetic-pharmacodynamic model with intra- and interindividual aspects. J Pharm Exp Ther 1995;274:921–927.
62. Lima JJ, Matsushima N, Kissoon N, *et al*. Modeling the metabolic effect of terbutaline in β 2-adrenergic receptor diplotypes. Clin Pharmacol Ther 2004;76:27–37.
63. Oosterhuis RJM, Berge T, Sauerwein HPE, *et al*. Pharmacokinetic-pharmacodynamic modeling of prednisolone induced lymphocytopenia in man. J Pharmacol Exp Ther 1984;229:539–546.
64. Derendorf H, Mollmann H, Krieg M, *et al*. Pharmacodynamics of methylprednisolone phosphate after single intravenous administration to healthy volunteers. Pharm Res 1991;8:263–268.
65. Gupta SK, Ritchie JC, Ellinwood EG, *et al*. Modeling the pharmacokinetics and pharmacodynamics of dexamethasone in depressed patients. Eur J Clin Pharmacol 1992;43:51–55.
66. Sharma A, Jusko WJ. Characteristics of indirect pharmacodynamic models. Brit J Pharm 1998;45:229–239.
67. Krzyzanski W, Jusko WJ. Mathematical formalism for the properties of four basic models of indirect pharmacodynamic responses. J Pharmacokinet Biopharm 1997;25(1):107–123.
68. Krzyzanski W, Ramakrishnan R, Jusko WJ. Basic pharmacodynamic models for agents that alter production of natural cells. J Pharmacokinet Biopharm 1999;27(5):467–489.
69. Ramakrishnan R, Cheung WK, Wacholtz MC, *et al*. Pharmacokinetic and pharmacodynamic modeling of recombinant human erythropoietin after single and multiple doses in healthy volunteers. J Clin Pharm 2004;44(9):991–1002.
70. Ramakrishnan R, Cheung WK, Farrell F, *et al*. Pharmacokinetic and pharmacodynamic modeling of recombinant human erythropoietin after intravenous and subcutaneous dose administration in cynomolgus monkeys. J Pharm Exp Ther 2003;306(1):324–331.
71. Woo S, Krzyzanski W, Duliege AM, *et al*. Population pharmacokinetics and pharmacodynamics of peptidic erythropoiesis receptor agonist (ERA) in healthy volunteers. J Clin Pharmacol 2008;48(1):43–52.
72. Woo S, Krzyzanski W, Jusko WJ. Target-mediated pharmacokinetic and pharmacodynamic model of recombinant human erythropoietin (rHuEPO). J Pharmacokinet Pharmacodyn 2007;34(6):849–868.
73. Woo S, Krzyzanski W, Jusko WJ. Pharmacodynamic model for chemotherapy-induced anemia in rats. Cancer Chemother Pharmacol 2008;62(1):123–133.
74. Woo S, Krzyzanski W, Jusko WJ. Pharmacokinetic and pharmacodynamic modeling of recombinant human erythropoietin after intravenous and subcutaneous administration in rats. J Pharmacol Exp Ther 2006;319(3):1297–306.

75. Krzyzanski W, Woo S, Jusko WJ. Pharmacodynamic models for agents that alter production of natural cells with various distributions of lifespans. J Pharmacokinet Pharmacodyn 2006;33(2):125–166.
76. Krzyzanski W, Perez-Ruixo JJ, Vermeulen A. Basic pharmacodynamic models for agents that alter the lifespan distribution of natural cells. J Pharmacokinet Pharmacodyn 2008;35(3):349–377.
77. Ramakrishnan R, DuBois DC, Almon RR, *et al*. Fifth-generation model for corticosteroid pharmacodynamics: application to steady-state receptor down-regulation and enzyme induction patterns during seven-day continuous infusion of methylprednisolone in rats. J Pharmacokinet Pharmacodyn 2002;29(1):1–24.
78. Mager DE, Jusko WJ. Pharmacodynamic modeling of time-dependent transduction systems. Clin Pharmacol Ther 2001;70(3):210–216.
79. Sun YN, Jusko WJ. Transit compartments versus gamma distribution function to model signal transduction processes in pharmacodynamics. J Pharm Sci 1998;87(6):732–737.
80. Perlstein I, Stepensky D, Krzyzanski W, *et al*. A signal transduction pharmacodynamic model of the kinetics of parasympathomimetic activity of low-dose scopolamine and atropine in rats. J Pharm Sci 2002;91(12):2500–2510.
81. Lobo ED, Balthasar JP. Pharmacodynamic modeling of chemotherapeutic effect: application of a transit compartment model to characterize methotrexate effects in-vitro. AAPS Pharm Sci 2002;4(4):1–11.
82. Simeoni M, Magni P, Cammia C, *et al*. Predictive pharmacokinetic-pharmacodynamic modeling of tumor growth kinetics in xenograft models after administration of anticancer agents. Cancer Res 2004;64:1094–1101.
83. Friberg LE, Henningsson A, Maas H, *et al*. Model of chemotherapy-induced myelosuppression with parameter consistency across drugs. J Clin Oncol 2002;20(24): 4713–4721.
84. Harker LA, Roskos LK, Marzec UM, *et al*. Effects of megakaryocyte growth and development factor on platelet production, platelet life span, and platelet function in healthy human volunteers. Blood 2000;95(8):2514–2522.
85. Xu L, Eiseman JL, Egorin MJ, *et al*. Physiologically-based pharmacokinetics and molecular pharmacodynamics of 17-(allylamino)-17-demethoxygeldanamycin and its active metabolite in tumor-bearing mice. J Pharmacokinet Pharmacodyn 2003;30(3):185–219.
86. Jusko WJ. Pharmacodynamics of chemotherapeutic effects: dose-time-response relationships for phase-nonspecific agents. J Pharm Sci 1971;60(6):892–895.
87. Zhi JG, Nightingale CH, Quintiliani R. Microbial pharmacodynamics of piperacillin in neutropenic mice of systematic infection due to *Pseudomonas aeruginosa*. J Pharmacokinet Biopharm 1988;16(4):355–375.
88. Mager DE, Jusko WJ. Mechanistic pharmacokinetic/pharmacodynamic models II. In: Williams PJ, Ette EI, editors. Pharmacometrics. New York: John Wiley and Sons, Inc.; 2007. pp. 607–631.
89. Ferron GM, Mckeand W, Mayer PR. Pharmacodynamics of irreversible effect on gastric acid secretion in human and rats. J Clin Pharmacol 2001;41:149–156.
90. Yamamoto K, Abe M, Katashima M, *et al*. Pharmacodynamic analysis of antiplatelet effect of aspirin in the literature—modeling cyclooxygenase in the platelet and the vessel wall endothelium. Jpn J Hospital Pharm 1996;22:133–141.
91. Holford NH, Sheiner LB. Understanding the dose-effect relationship: clinical application of pharmacokinetic-pharmacodynamic models. Clin Pharmacokinet 1981;6(6): 429–453.
92. Mould DR. Developing models of disease progression. In: Williams PJ, Ette EI, editors. Pharmacometrics. New York: John Wiley and Sons, Inc.; 2007. pp. 547–581.
93. Chan PLS, Holford NHG. Drug treatment effects on disease progression. Annu Rev Pharmacol Toxicol 2001;41:625–659.

94. Holford NHG, Peace KE. Results and validation of a population pharmacodynamic model for cognitive effects in Alzheimer patients treated with tacrine. Proc Natl Acad Sci U S A 1992;89:11471–11475.
95. Sharma A, Ebling WF, Jusko WJ. Precursor-dependent indirect pharmacodynamic response model for tolerance and rebound phenomena. J Pharm Sci 1998;87(12):1577–1584.
96. Bauer JA, Fung HL. Pharmacodynamic models of nitroglycerine-induced hemodynamic tolerance in experimental heart. Pharm Res 1994;11:816–823.
97. Wakelkamp M, Alvan G, Gabrielson J, *et al*. Pharmacodynamic modeling of furosemide tolerance after multiple intravenous administration. Clin Pharmacol Ther 1996;60:75–88.
98. WinNonlin, Professional ed. version 5.2, Pharsight Corp., 800 West Elcamino Real, Suite 200, Mountain View CA 94040.
99. D'Argenio DZ, Schumitzky A, Wang X. ADAPT 5 user's guide: pharmacokinetic/pharmacodynamic systems analysis software. Biomedical Simulations Resource, Los Angeles. 2009.
100. Macey RI, Oster GF. Berkeley Madonna, version 8.0. University of California at Berkeley, Berkeley, Calif. 2001.
101. GraphPad Prism version 5.00 for Windows, GraphPad Software, San Diego California USA. Available at www.graphpad.com.
102. D'Argenio DZ, Mager DE. Bridging pharmacology and pathophysiology via systems modeling. J Clin Pharmacol 2010;50(9 Suppl):56 S–57 S.
103. Athanasiades A, Ghorbel F, Clark JW Jr, *et al*. Energy analysis of a nonlinear model of the normal human lung. J Biol Syst 2000;8(2):115–139.
104. Jung E, Lee W. Lumped parameter models of cardiovascular circulation in normal and arrhythmia cases. J Korean Math Soc 2006;43(4):885–897.
105. Landersdorfer CB, Jusko WJ. Pharmacokinetic/pharmacodynamic modelling in diabetes mellitus. Clin Pharmacokinet 2008;47:417–448.
106. Post TM, Freijer JI, DeJongh J, *et al*. Disease system analysis: basic disease models in degenerative disease. Pharm Res 2005;22:1038–1049.
107. Quantitative and systems pharmacology in the post-genomic era: new approaches to discovering drugs and understanding therapeutic mechanisms. An NIH white paper by the QSP Workshop Group; 2011. Available at http://www.nigms.nih.gov/NR/rdonlyres/8ECB1F7C-BE3B-431F-89E6-A43411811AB1/0/SystemsPharmaWPSorger2011.pdf.